

# Quantifying Model Risk in Option Pricing and Value-at-Risk Models

Dumisani Ngwenza

A dissertation submitted to the Faculty of Commerce, University of Cape Town, in partial fulfilment of the requirements for the degree of Master of Philosophy.

September 14, 2019

*MPhil in Mathematical Finance,  
University of Cape Town.*



The copyright of this thesis vests in the author. No quotation from it or information derived from it is to be published without full acknowledgement of the source. The thesis is to be used for private study or non-commercial research purposes only.

Published by the University of Cape Town (UCT) in terms of the non-exclusive license granted to UCT by the author.

# Declaration

I declare that this dissertation is my own, unaided work. It is being submitted for the Degree of Master of Philosophy to the University of Cape Town. It has not before been submitted for any degree or examination.

Signed by candidate
---------------------

---

Name Surname

September 14, 2019

# Abstract

Financial practitioners use models in order to price, hedge and measure risk. These models are reliant on assumptions and are prone to "model risk". Increased innovation in complex financial products has lead to increased risk exposure and has spurred research into understanding model risk and its underlying factors. This dissertation quantifies model risk inherent in Value-at-Risk (VaR) on a variety of portfolios comprised of European options written on the ALSI futures index across various maturities. The European options under consideration will be modelled using the Black-Scholes, Heston and Variance-Gamma models.

# Acknowledgements

I would like to acknowledge Obeid Mahomed and Associate Professor Peter Ouwehand for the guidance, patience and invaluable input. I would also like to Associate Professor David Taylor for helping me during the writing period. Lastly I am grateful for the support and patience from the AIFMRM department, classmates, friends and family.

# Contents

<b>1. Introduction</b>	1
<b>2. Model Risk</b>	3
2.1 Model Risk Classification	3
2.2 Model Risk Quantification	4
2.3 Robust Monte Carlo	6
<b>3. Option Pricing Models</b>	7
3.1 The Black-Scholes model	7
3.2 The Heston Stochastic Volatility model	8
3.3 The Variance-Gamma Model	9
<b>4. Model Calibration</b>	11
4.1 Data	11
4.2 Black-Scholes Calibration	12
4.3 Heston Model Calibration	13
4.4 Variance-Gamma Calibration	15
<b>5. Static Hedging and VaR</b>	18
5.1 Path Simulation	18
5.1.1 Bootstrap Method	18
5.1.2 Risk-Neutral simulation	19
5.2 Static Hedging	20
5.3 VaR	23
<b>6. Results</b>	25
6.1 Profit and Loss Distributions	25
6.2 VaR model risk	28
<b>7. Discussion and Conclusion</b>	34
<b>Bibliography</b>	36
<b>A. Preliminaries</b>	38
A.1 Definitions	38
A.2 Lagrangian Duality	38

<b>B. Appendix B</b> . . . . .	40
B.1 Profit and Loss Distributions . . . . .	40
B.2 VaR Results . . . . .	48

# List of Figures

4.1	Comparison of Black-Scholes and market implied call option prices across various days-to-maturities. . . . .	12
4.2	Market implied volatility smile, Heston volatility smile and BS constant volatility across various days-to-maturities. . . . .	14
4.3	Comparison of Heston and market implied call option prices across various days-to-maturities. . . . .	15
4.4	Market implied volatility smile, VG volatility smile and BS constant volatility across various days-to-maturities. . . . .	16
4.5	Comparison of VG and market implied call option prices across various days-to-maturities. . . . .	17
5.1	Distribution of $S_{t_{10}}$ under Historical Bootstrap, Black-Scholes, Heston and Variance Gamma assumptions after 10 days. . . . .	20
5.2	$\Delta_C$ for BS, Heston and VG at time $t_0$ . . . . .	22
6.1	ATM call P&L distributions for BS, Heston and VG 90 with days-to-maturity. . . . .	26
6.2	Long-only portfolio P&L distributions for BS, Heston and VG with 90 days-to-maturity. . . . .	27
6.3	Collar portfolio P&L distributions for BS, Heston and VG models with 90 days-to-maturity. . . . .	27
6.4	ATM Nominal and Perturbed MC 95% VaR . . . . .	30
6.5	Long-only Nominal and Perturbed MC 95% VaR . . . . .	32
6.6	Collar Nominal and Perturbed MC 95% VaR . . . . .	33
B.1	ATM portfolio nominal and perturbed P&L Distributions for the BS, Heston and VG models 30 days-to-maturity options. . . . .	40
B.2	Long-only portfolio nominal and perturbed P&L Distributions for the BS, Heston and VG models 30 days-to-maturity options. . . . .	41
B.3	Collar portfolio nominal and perturbed P&L Distributions for the BS, Heston and VG models 30 days-to-maturity options. . . . .	42
B.4	ATM portfolio perturbed P&L Distributions for the Black-Scholes (BS), Heston and VG models 180 days-to-maturity options. . . . .	43
B.5	Long-only portfolio perturbed P&L Distributions for the Black-Scholes (BS), Heston and VG models 180 days-to-maturity options. . . . .	44
B.6	Collar portfolio perturbed P&L Distributions for the Black-Scholes (BS), Heston and VG models 180 days-to-maturity options. . . . .	45



B.7	ATM portfolio perturbed P&L Distributions for the Black-Scholes (BS), Heston and VG models 270 days-to-maturity options. . . . .	46
B.8	Long-only portfolio perturbed P&L Distributions for the Black-Scholes (BS), Heston and VG models 270 days-to-maturity options. . . . .	47
B.9	Collar portfolio perturbed P&L Distributions for the Black-Scholes (BS), Heston and VG models 270 days-to-maturity options. . . . .	48

# List of Tables

4.1	Black-Scholes (BS) calibration results. . . . .	12
4.2	Heston model calibration results . . . . .	14
4.3	VG calibrated parameters . . . . .	16
6.1	10-day VaR of portfolios with $\tau = 90$ days-to-maturity . . . . .	28
B.1	10-day VaR of portfolios with $\tau = 30$ days-to-maturity . . . . .	48
B.3	10-day VaR of portfolios with $\tau = 270$ days-to-maturity . . . . .	49
B.2	10-day VaR of portfolios with $\tau = 180$ days-to-maturity . . . . .	49

## Chapter 1

# Introduction

Financial risk measurement is a fundamental practice that relies on the use of models and market information for pricing, hedging, reserving and regulatory purposes. The models are often heavily reliant on a variety of assumptions and are thus themselves a source of what is referred to as “model risk”. Model risk was identified as a key component of the financial crisis of 2008/9. With an increase in risk exposure from both the number and complexity of financial products and their models, quantifying model risk is imperative.

[Derman \(1996\)](#) investigates some properties of model risk, in particular discerning the factors that introduce risk in any model. [Detering and Packham \(2016\)](#) evaluate the intrinsic model risk in Value-at-Risk (VaR) and Expected Shortfall when distributional losses are generated by model-dependent hedging. [Kerkhof \*et al.\* \(2010\)](#) evaluates model risk by directly integrating the model error into VaR. [Schlögl \(2016\)](#) presents a framework in which model error is classified into four categories of risk factors. This framework is essential when distinguishing factors that affect model risk for pricing, hedging or risk measurement.

This dissertation evaluates the model risk in market risk capital charge for a variety of portfolios of European options, using VaR as the risk metric. VaR is concisely defined as the expected loss of a portfolio, with a certain level of confidence over a period of time. We evaluate VaR in a model-dependent manner where the profit and loss (P&L) is determined by static delta hedging. VaR is then interpreted as the expected loss if the portfolio cannot be hedged over a certain period of time.

In this context, we choose to quantify model risk using the methodology of [Glasserman and Xu \(2014\)](#). This methodology continues the work of [Hansen and Sargent \(2008\)](#), which is based on the [Kullback and Leibler \(1951\)](#) divergence (also referred to as relative entropy). The Kullback-Leibler (KL) divergence measures the additional information required in order for an alternative model to be preferable to a nominal model. By comparing a nominal model to a (possibly) preferable alternative, KL divergence is the foundation for quantifying model risk.

The VaR models we consider are the Historical VaR, as the nominal model, and the Monte Carlo VaR, as the alternative model. These are determined on three portfolios consisting of SAFEX (South African Futures Exchange) European options written on ALSI (All Share Index) futures contracts. The analysis of VaR on three different portfolios will determine whether Monte Carlo VaR and Historical VaR are commensurate. This is crucial for regulatory purposes. A commensurate Monte Carlo VaR may permit the quantification of model risk on market risk capital charges for exotic portfolios. Historical data on these might not be available, hence invalidating Historical VaR.

The three different portfolios that will be analysed consist of a long position in an at-the-money (ATM) call option, a long-only portfolio with three call options of various moneyness, and a collar portfolio consisting of a short position in an out-the-money (OTM) call option, a long position in an OTM put option and a long position in the underlying ALSI futures contract. These are all analysed over various times-to-maturity. The option pricing models used to value the SAFEX European options will be [Black and Scholes \(1973\)](#), which assumes a constant volatility, the [Heston \(1993\)](#) Stochastic Volatility model, which aims to reproduce the volatility smile, and the Variance Gamma model pioneered by [Madan \*et al.\* \(1998\)](#), which assumes market information is known at random times.

The rest of the dissertation is as follows. Chapter 2 gives an overview of the model risk methodology of [Glasserman and Xu \(2014\)](#). In particular, the role of the KL divergence, which forms the foundation for quantifying the worst-case model error, and the robust Monte Carlo approach to estimating model error will be discussed. Chapter 3 explores the stochastic models that will be applied in the valuation of the SAFEX European options. A discussion of the calibration of these models follows in Chapter 4. Chapter 5 gives an overview of the Historical and Monte Carlo VaR models and the delta hedging methodology used to obtain the profit and loss distributions. Chapter 6 presents the results for model error. Chapter 7 concludes with a discussion of the results and possible extensions.

## Chapter 2

# Model Risk

In order to compare models, a tool is required to measure their disparity. The work of [Glasserman and Xu \(2014\)](#) on model error relies on the use of the [Kullback and Leibler \(1951\)](#) divergence (or relative entropy) to measure this disparity. This chapter begins by defining model risk and discussing a framework developed by [Schlögl \(2016\)](#) on the classification of model risk. This is followed by the quantification of model risk, beginning with the definition of the Kullback-Leibler divergence and a brief overview of its properties. This is followed by a discussion of model risk and the robust Monte Carlo approach based on the work of [Glasserman and Xu \(2014\)](#).

### 2.1 Model Risk Classification

The use of financial models are heavily reliant on assumptions and are a source of risk. This risk is termed "model risk" and has led research on its quantification. [Schlögl \(2016\)](#) presents a general framework that classifies model risk into four categories:

1. Type 0 describes the risk of the model associated with parameters. This includes risk of parameter sensitivity that is a result of parameter misspecification. Type 0 arises due to a lack of information in liquidly traded market instruments.
2. Type 1 is the inability of the model to recover a complete set of market observations. Type 1 is referred to as calibration error - the inability to recover the market observations, irrespective of the model's dynamics.
3. Type 2 is the risk incurred as a result of recalibration error. This error is a contradiction of the model assumptions (due to the lack of parameter stability). Over time, the model needs to be recalibrated in order to have an accurate fit.

The frequent calibrations are a violation of the model's assumption of fixed parameters.

4. Type 3 describes the contradiction of the model assumptions with its empirical dynamics. This is as a result of a misspecification of the stochastic dynamics.

Using this framework will enable us to discern the factors affecting model risk in the quantification of model risk in Value-at-Risk models.

## 2.2 Model Risk Quantification

We begin by defining the [Kullback and Leibler \(1951\)](#) divergence and thereafter give a brief overview of model risk according to [Glasserman and Xu \(2014\)](#).

**Definition 2.1.** The Kullback-Leibler (KL) divergence between the nominal distribution  $dQ$ , and the alternative distribution  $dP$ , is defined as,

$$D(Q||P) = \int \log \left( \frac{dQ}{dP} \right) dQ.$$

**Definition 2.2.** The KL divergence has the following properties:

- i.  $D(Q||P) \geq 0$ .
- ii.  $D(Q||P) = 0$  if and only if  $dQ = dP$  almost everywhere.
- iii.  $D(Q||P) \neq D(P||Q)$ .

Note that  $D(Q||P)$  is not a metric. Although it measures the "distance" between two disparate distributions,  $D(Q||P)$  is not symmetric. That is, property iii of Definition 2.2 does not satisfy property iii of a metric in Definition A.1. However, properties i and ii of the KL divergence satisfies properties i and ii of a metric (defined in Definition A.1). Despite this, the KL divergence has attractive properties inherent to a metric and can be considered as a pseudo-metric. It should be noted that [Glasserman and Xu \(2014\)](#) do not view  $dQ$  and  $dP$  as symmetric distributions and we consider the possibility of  $dP$  as a more suitable distribution although  $dQ$  might be the favoured distribution.

[Glasserman and Xu \(2014\)](#) use the KL divergence in order to quantify the "distance" between two distributions. This requires the selection of a nominal distribution, to which the alternative distribution will be compared. This pseudo-metric measures the information gained that would make the alternative distribution preferable.

Model risk, defined by [Glasserman and Xu \(2014\)](#), is classified as the worst-case error for a risk measure  $V(X)$  on the random variable  $X$ . In our context, the risk measure  $V(X)$  denotes Value-at-Risk (VaR) on a portfolio of European options. In order to quantify model risk, consider alternative models that are a "distance" of  $\eta$  from the nominal model, where  $\eta$  is termed the relative entropy budget. The alternative models are described by the set  $\mathcal{P}_\eta$  of Radon-Nikodym derivatives  $m(X)$  such that,

$$\mathbb{E}[m(X) \log m(X)] < \eta.$$

Suppose the Radon-Nikodym derivatives are given by  $m = \frac{dQ}{dP}$ , which assumes, without loss of generality, that  $dP > 0$ . Further suppose that  $Q_X, P_X$  have densities  $f$  and  $\tilde{f}$  respectively. The expectation of  $V(X)$  under the alternative distribution  $dP$  is,

$$\tilde{\mathbb{E}}[V(X)] = \mathbb{E}[m(X)V(X)] = \int m(x)V(x)f(x)dx = \int V(x)\tilde{f}(x)dx. \quad (2.1)$$

It follows that the worst-case lower and upper bounds are given by,

$$\inf_{m \in \mathcal{P}_\eta} \mathbb{E}[m(X)V(X)] \quad \text{and} \quad \sup_{m \in \mathcal{P}_\eta} \mathbb{E}[m(X)V(X)], \quad (2.2)$$

respectively. In order to determine the maximisation problem in Equation (2.2), the primal is given by <sup>1</sup>,

$$- \inf_{m \in \mathcal{P}_\eta} \mathbb{E}[-m(X)V(X)] \quad \text{subject to} \quad \mathbb{E}[m(X) \log(m(X))] - \eta \leq 0. \quad (2.3)$$

In this context, the function that is to be minimised,  $g(m) = \mathbb{E}[-m(X)V(X)]$ , is linear in  $m$  and thus convex. The constraint,  $h(m) = \mathbb{E}[m(X) \log(m(X))] - \eta$  is also convex. Thus the minimisation approach to equation (2.3) is given by the following,

$$\inf_{\delta > 0} \sup_m \mathbb{E} \left[ m(X)V(X) - \frac{1}{\delta} \left( m(X) \log m(X) - \eta \right) \right]. \quad (2.4)$$

[Glasserman and Xu \(2014\)](#) state that, with the Lagrangian multiplier  $\delta$  being strictly positive, the worst possible risk within the distance  $\eta$  will be given by,

$$\inf_{\delta > 0} \sup_{m \in \mathcal{P}_\eta} \mathbb{E} \left[ m(X)V(X) - \frac{1}{\delta} \left( m(X) \log m(X) - \eta \right) \right],$$

with,

---

<sup>1</sup> See Appendix A.2 for an explication of the Lagrangian duality

$$m(X) = \frac{\exp(\delta V(X))}{\mathbb{E}[\exp(\delta V(X))]}.$$

Similarly, the lower bound is solved with  $\delta$  being strictly negative. The worst-case model error is characterised by an exponential change of measure which is defined in terms of the risk measure  $V(X)$  and the parameter  $\delta$ .

## 2.3 Robust Monte Carlo

[Glasserman and Xu \(2014\)](#) describe a robust Monte Carlo approach that estimates model risk.

Consider the problem  $\sup_{m \in \mathcal{P}_\eta} \mathbb{E}[m(X)V(X)]$ , where the dual optimisation is described by Equation (2.4). The inner supremum has a solution of the form,

$$m_\delta(X) = \frac{e^{\delta V(X)}}{\mathbb{E}[e^{\delta V(X)}]}.$$

Suppose independent replications  $X_1, X_2, \dots, X_N$  of the random element  $X$  is generated. The Monte Carlo estimate of  $\mathbb{E}[V(X)]$  is determined by,

$$\frac{1}{N} \sum_{i=1}^N V(X_i).$$

For a given  $\delta$  and the Radon-Nikodym derivative  $m_\delta \propto e^{\delta V(X)}$ , the expectation of  $V(X)$  can be estimated using the change of measure  $m_\delta$ , determined by  $X_i$  under the nominal measure. The estimator,

$$\tilde{\mathbb{E}}[V(X)] = \mathbb{E}[m(X)V(X)] = \frac{\sum_{i=1}^N V(X_i)e^{\delta V(X_i)}}{\sum_{i=1}^N e^{\delta V(X_i)}}, \quad (2.5)$$

converges to  $\mathbb{E}[m_\delta(X)V(X)]$  as  $N \rightarrow \infty$ . With the same generated replications, the Radon-Nikodym derivative can be estimated by,

$$\hat{m}_{\delta,i} = \frac{e^{\delta V(X_i)}}{\frac{1}{N} \sum_{j=1}^N e^{\delta V(X_j)}}, \quad i = 1, \dots, N. \quad (2.6)$$

Then, estimation of the relative entropy of  $m_\delta$  is given by,

$$\hat{\eta}(\delta) = \frac{1}{N} \sum_{i=1}^N \hat{m}_{\delta,i} \log \hat{m}_{\delta,i}. \quad (2.7)$$

By varying  $\delta$ , the risk measure  $V(X)$ , under various exponential change of measures  $m_\delta$ , can be estimated and an optimal  $\delta$  can be selected where,

$$\mathbb{E}[\hat{m}_\delta \log \hat{m}_\delta] < \hat{\eta}(\delta) \leq \eta.$$



## Chapter 3

# Option Pricing Models

In this chapter we give a brief overview of the models we considered for option pricing: the Black-Scholes model ([Black and Scholes \(1973\)](#)), which assumes a constant volatility, the Heston Stochastic Volatility model ([Heston \(1993\)](#)), which reproduces the volatility smile, and the Variance-Gamma model ([Madan \*et al.\* \(1998\)](#)), which assumes information is known at random times. Options are written on the ALSI (All Share Index) Futures index.

### 3.1 The Black-Scholes model

The Black-Scholes model for European options assumes that the stock price process follows Geometric Brownian Motion (GBM). Assume a risk-neutral setting  $(\Omega, \mathcal{F}, \mathbb{Q})$ , with market information  $(\mathcal{F}_t)_{t \geq 0}$  at time  $t$ . The risk-neutral stock price process dynamics are,

$$dS_t = rS_t dt + \sigma_{BS} S_t dW_t, \quad (3.1)$$

where  $r$  is the risk-free rate of return,  $\sigma_{BS} > 0$  is the constant volatility of the underlying  $S_t$ , and  $W_t$  is the  $\mathbb{Q}$ -Brownian motion. The corresponding Black-Scholes (BS) price for a European call option is,

$$c_t^{BS} = S_t N(d_+) - K e^{-r\tau} N(d_-), \quad (3.2)$$

where  $N(\cdot)$  denotes the cumulative standard normal distribution,  $K$  is the strike price,  $(S_t)_{t \geq 0}$  is the stock price process, the expiry date is  $T$  and the time-to-maturity is  $\tau = T - t$ .

$$d_+ = \frac{\log(S_t/K) + (r + 0.5\sigma_{BS}^2)\tau}{\sigma_{BS}\sqrt{\tau}}, \quad d_- = d_+ - \sigma_{BS}\sqrt{\tau}. \quad (3.3)$$

## 3.2 The Heston Stochastic Volatility model

The Heston Stochastic Volatility model (Heston (1993)), allows the volatility of the stock price process to change stochastically. Contrary to the Black-Scholes model, the volatility of the underlying is described by a diffusion process. This characteristic allows the Heston model to reproduce the volatility smile.

In a risk-neutral setting  $(\Omega, \mathcal{F}, \mathbb{Q})$ , with the filtration  $(\mathcal{F}_t)_{t \geq 0}$ , which represents the market information at time  $t$ , the stock price process is given by,

$$\begin{aligned} dS_t &= rS_t dt + \sqrt{v_t} S_t dW_t \\ dv_t &= \kappa(\theta_H - v_t)dt + \sigma_H \sqrt{v_t} dB_t, \end{aligned} \quad (3.4)$$

where  $r$  is the risk-free rate of return, the instantaneous variance  $v_t$  with  $v_0 \geq 0$ , the mean-reversion speed  $\kappa > 0$ , the mean-reversion level  $\theta_H > 0$  and volatility of the volatility process  $\sigma_H > 0$ . The instantaneous volatility,  $(v_t)_{t \geq 0}$ , follows the Cox *et al.* (1985) interest rate term structure.  $W_t$  and  $B_t$  are dependent  $\mathbb{Q}$ -standard Brownian motions such that  $d\langle W_t, B_t \rangle = \rho dt$ , where  $\rho \in [-1, 1]$  is the correlation between the Brownian motions. The set  $\Theta_{Heston} = \{v_0, \theta_H, \rho, \kappa, \sigma_H\}$  is considered the set of Heston models parameters.

If Feller's condition, defined as  $2\kappa\theta_H > \sigma_H^2$ , is met then the volatility process will be strictly positive.

Define  $X_t = \log S_t$ . The dynamics of the log-price process  $X_t$  follows from Itô's formula as,

$$dX_t = \left(r - \frac{v_t}{2}\right)dt + \sqrt{v_t}dW_t. \quad (3.5)$$

The characteristic function provided by Albrecher *et al.* (2007) is given by,

$$\phi_{Heston}(u, \tau) = \exp[C(\tau, u) + D(\tau, u) \cdot v_0 + iux_0], \quad (3.6)$$

where  $X_0 = x_0$  is the known log-price at time  $t = 0$ , and,

$$\begin{aligned} C(\tau, u) &= iur\tau + \frac{\kappa\theta_H}{\sigma_H^2} \left[ (\kappa - iu\rho\sigma_H - d)\tau - 2\log\left(\frac{1 - ge^{-d\tau}}{1 - g}\right) \right], \\ D(\tau, u) &= \frac{\kappa - iu\rho\sigma_H - d}{\sigma_H^2} \cdot \frac{1 - e^{-d\tau}}{1 - g \cdot e^{-d\tau}}, \\ g &= \frac{\kappa - iu\rho\sigma_H - d}{\kappa - iu\rho\sigma_H + d}, \\ d &= \sqrt{(iu\rho\sigma_H - \kappa)^2 + \sigma_H^2(iu + u^2)}. \end{aligned} \quad (3.7)$$

The price of a European call option under these dynamics (Gil-Pelaez (1951)) is given by,

$$c^H(S_t, K, \tau) = S_0 P_1 - K e^{-r\tau} P_2,$$

$$\text{Where } P_1 = \frac{1}{2} + \frac{1}{\pi} \int_0^\infty \operatorname{Re} \left[ \frac{e^{-iu \ln(K)} \phi_{Heston}(u - i, \tau)}{iu \phi_{Heston}(-i, \tau)} \right] du, \quad (3.8)$$

$$P_2 = \frac{1}{2} + \frac{1}{\pi} \int_0^\infty \operatorname{Re} \left[ \frac{e^{-iu \ln(K)} \phi_{Heston}(u, \tau)}{iu} \right] du$$

where  $K$  is the strike price,  $r$  is the risk-free rate of return,  $\tau$  is the time-to-maturity and  $\phi_{Heston}(\cdot, \tau)$  is the characteristic function of the log-price at the time of expiry,  $T$ .

### 3.3 The Variance-Gamma Model

The Variance-Gamma model (VG)(Madan *et al.* (1998)) is obtained via a Brownian motion with constant drift and volatility. The VG model assumes that market information is obtained at random times. This random time change is modelled using a gamma process. Each unit of time is given by an independent random variable that is driven by a gamma density with a unit mean and positive variance,  $\nu$ .

In order to obtain the European The VG process is obtained by evaluating the Brownian motion  $b(t; \theta_{VG}, \sigma_{VG})$  given by,

$$db(t; \theta_{VG}, \sigma_{VG}) = \theta_{VG} dt + \sigma_{VG} dW_t,$$

with the drift  $\theta_{VG}$ , volatility  $\sigma_{VG}$  at a random time modelled by the gamma process and  $W_t$  is a standard Brownian motion.

The VG process,  $X(t; \sigma_{VG}, \nu, \theta_{VG})$ , is obtained in terms of a Brownian motion with drift  $b(t; \theta_{VG}, \sigma_{VG})$  and gamma process with a unit mean rate  $y(t; 1, \nu)$  given as:

$$X(t; \sigma_{VG}, \nu, \theta_{VG}) = b(y(t; 1, \nu); \theta_{VG}, \sigma_{VG}). \quad (3.9)$$

The risk-neutral stock prices are given by,

$$S_t = S_0 \exp((r + \omega)t + X(t; \sigma_{VG}, \nu, \theta_{VG})),$$

The characteristic function of the VG model is given by (Carr and Madan (1999)),

$$\begin{aligned} \phi_{VG}(u, \tau) = & \exp[iu(\log S_0 + (\theta_{VG} + \omega - \frac{1}{2}\sigma_{VG}^2)\tau)] \times \\ & \phi_{X_t}(u, \tau) \exp\left[-\frac{1}{2}(u\sigma_{VG})^2\tau\right], \end{aligned} \quad (3.10)$$

where  $\omega = \frac{1}{\nu} \ln(1 - \theta_{VG}\nu - 0.5\sigma_{VG}^2\nu)$  and  $\phi_{X_t}$  is given by,

$$\phi_{X_t}(u, t) = \left( \frac{1}{1 - iu\nu\theta_{VG} + 0.5\nu(u\sigma_{VG})^2} \right)^{\frac{t}{\nu}} \quad (3.11)$$

Equation (3.10) can be used to derive the price of a European call option,

$$\begin{aligned} c^{VG}(S_t, K, \tau) = & S_0 P_1 - K e^{-r\tau} P_2, \\ \text{Where } P_1 = & \frac{1}{2} + \frac{1}{\pi} \int_0^\infty \text{Re} \left[ \frac{e^{-iu \ln(K)} \phi_{VG}(u - i, \tau)}{iu \phi_{VG}(-i, \tau)} \right] du, \\ P_2 = & \frac{1}{2} + \frac{1}{\pi} \int_0^\infty \text{Re} \left[ \frac{e^{-iu \ln(K)} \phi_{VG}(u, \tau)}{iu} \right] du \end{aligned} \quad (3.12)$$

where  $\lambda > 0$  is a damping parameter that ensures integrability. All the other input parameters are as previously defined.  $\Theta_{VG} = \{\sigma_{VG}, \nu, \theta_{VG}\}$  is considered the set of VG model parameters.

The corresponding European put option price for the Black-Scholes, Heston and the VG models are obtained via put-call parity.

## Chapter 4

# Model Calibration

This chapter details the implementation of the Black-Scholes, Heston and VG SAFEX (South African Futures Exchange) European options written on the ALSI (All Share Index) Futures contracts. This is preceded by a description of the data.

Calibration of the option pricing models entails solving a constrained non-linear optimisation problem in order to determine the risk-neutral,  $\mathbb{Q}$ -measure, model parameters  $\Theta$  which best fits the market data. Optimisation requires the use of an objective function (or error measure) which can be defined in various ways, depending on the calibration instruments used. Calibration instruments refer to quoted option prices and implied volatilities.

For the sake of consistency, the same objective function is used for the Black-Scholes, Heston and VG calibration. The relative squared price error (RSPE) objective function ([Escobar and Gschnaidtner \(2016\)](#)) is defined as,

$$\text{RSPE} = \sum_{i=1}^{N_D} \left( \frac{c_i^{\text{Model}} - c_i^{\text{Market}}}{c_i^{\text{Market}}} \right)^2, \quad (4.1)$$

where  $N_D$  is the number of instruments used in the calibration.

Calibration on the various option pricing models is performed using *MATLAB*'s built-in *fmincon* optimisation function together with the *sqp* algorithm. Due to time and resource constraints, local minima were found.

### 4.1 Data

The data regarding SAFEX European options on ALSI futures contracts in the market is quoted in terms of implied volatilities. The ALSI index is comprised of 40 of the largest listed companies on the JSE, weighted by market capitalisation. Strikes range from 80% to 120% moneyness with increments of 5%. The maturities are {30, 90, 180, 270} days-to-maturity. The data ranges from 04 November 2008 to 29 June 2018. Due to the risk of using data that might be outdated, the data was

truncated to 1500 days, spanning from 25 June 2012 to 29 June 2018. Calibration of  $\sigma_{BS}$ ,  $\Theta_{Heston}$  and  $\Theta_{VG}$  is obtained using 20 days time series data from 25 June 2012.

## 4.2 Black-Scholes Calibration

The Black-Scholes model requires calibration of a single parameter, viz. the constant volatility  $\sigma_{BS}$ . The analytical Black-Scholes option price is given by equation (3.2). The Black-Scholes calibration results are given in Table 4.1. Figure 4.1 shows the calibrated Black-Scholes call option prices compared to the market implied call option prices.

	Days-to-maturity			
Parameters	30	90	180	270
$\sigma_{BS}$	20.50%	20.50%	21.35%	21.57%
RSPE	0.0032	0.0181	0.0345	0.0443

**Table 4.1:** Black-Scholes (BS) calibration results.

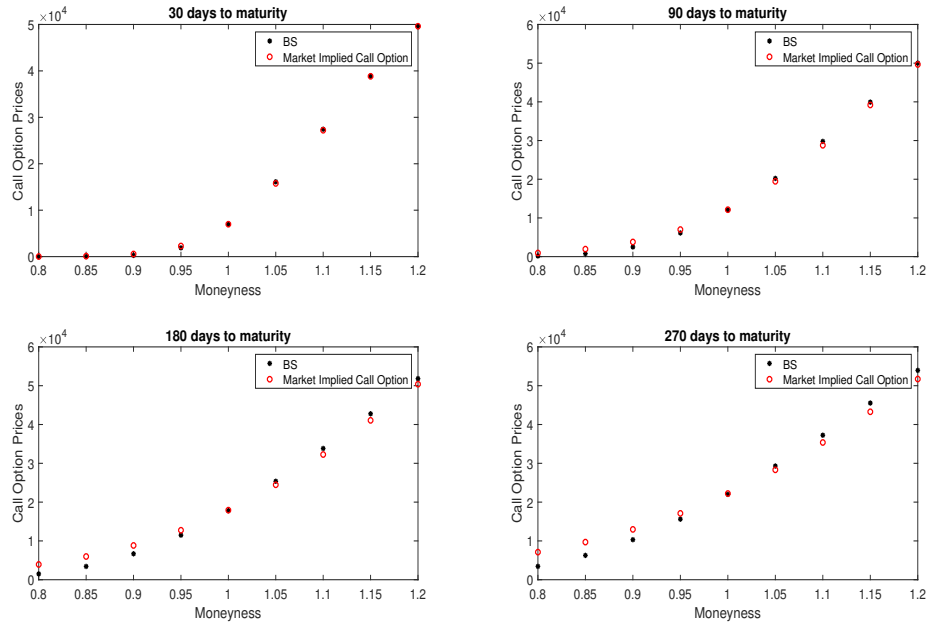


**Figure 4.1:** Comparison of Black-Scholes and market implied call option prices across various days-to-maturities.

Figure 4.1 shows how the calibrated Black-Scholes call option prices in compar-

ison to the market implied call prices. It can be seen that for options with longer time-to-maturity, the Black-Scholes assumption of a constant volatility does not recover the market implied call prices. This effect can be seen on options with 270 days-to-maturity.

### 4.3 Heston Model Calibration

Calibration of the Heston model requires determination of the five model parameters,  $\Theta_{Heston} = \{v_0, \theta_H, \rho, \kappa, \sigma_H\}$ . Semi-analytical formulae are available for the computation of the European call option prices. These are,

$$\begin{aligned} c_t^H(S_t, \tau) &= S_t P_1 - K e^{-r\tau} P_2 \\ \text{with } P_1 &= \frac{1}{2} + \frac{1}{\pi} \sum_{n=1}^N \text{Re} \left[ \frac{e^{-iu_n k} \phi_{Heston}(u_n - i, \tau)}{iu_n \phi_{Heston}(-i, \tau)} \right] \Delta u \\ P_2 &= \frac{1}{2} + \frac{1}{\pi} \sum_{n=1}^N \text{Re} \left[ \frac{e^{-iu_n k} \phi_{Heston}(u_n, \tau)}{iu_n} \right] \Delta u, \end{aligned} \quad (4.2)$$

where  $k = \ln(K)$ ,  $\Delta u = \frac{u_{max}}{N}$  and  $u_n = (n - \frac{1}{2})\Delta u$ . The integration limits are truncated to the interval  $[0, u_{max}]$ , where the upper integration limit is  $u_{max} = 30$  and the number of quadrature steps is  $N = 100$ .

The following specifications recommended by [Escobar and Gschnaidtner \(2016\)](#) were implemented,

Function Tolerance:	1e-10
Maximum Function Iterations:	10000
Maximum Iterations:	50000

With the following lower bound (lb) and upper bound (ub) constraints,

$$\begin{aligned} \text{lb: } & \{1\text{e-}5, 1\text{e-}5, -0.99, 1\text{e-}5, 1\text{e-}5\} \\ \text{ub: } & \{3, 3, 0.99, 20, 3\} \end{aligned}$$

The Heston calibration results are given in Table [4.2](#).

It should be noted that Feller's condition was not enforced during the calibration of the Heston model as either an initial guess or as a constraint. This is evident

	Days-to-maturity			
Parameters	30	90	180	270
$v_0$	0.0491	0.0847	0.2338	0.2838
$\theta_H$	0.0082	0.0335	0.0214	0.0278
$\rho$	0.988	0.7331	0.7434	0.7638
$\kappa$	1.1929	19.5812	15.1437	14.4774
$\sigma_H$	0.1742	0.9676	1.4246	1.8722
RSPE	0.001210689	0.00011962	1.29e-05	1.02e-06

Table 4.2: Heston model calibration results

in the resultant calibrated parameters as Feller's condition is not met for all days-to-maturity. According to Cui *et al.* (2017), relaxing Feller's condition is not always detrimental to modelling and may be beneficial for derivative pricing.

Figure 4.2 shows the Heston implied volatility smile compared to the market implied volatility smile and the Black-Scholes constant volatility. Figure 4.3 shows the Heston call option prices compared to the market implied call option prices.

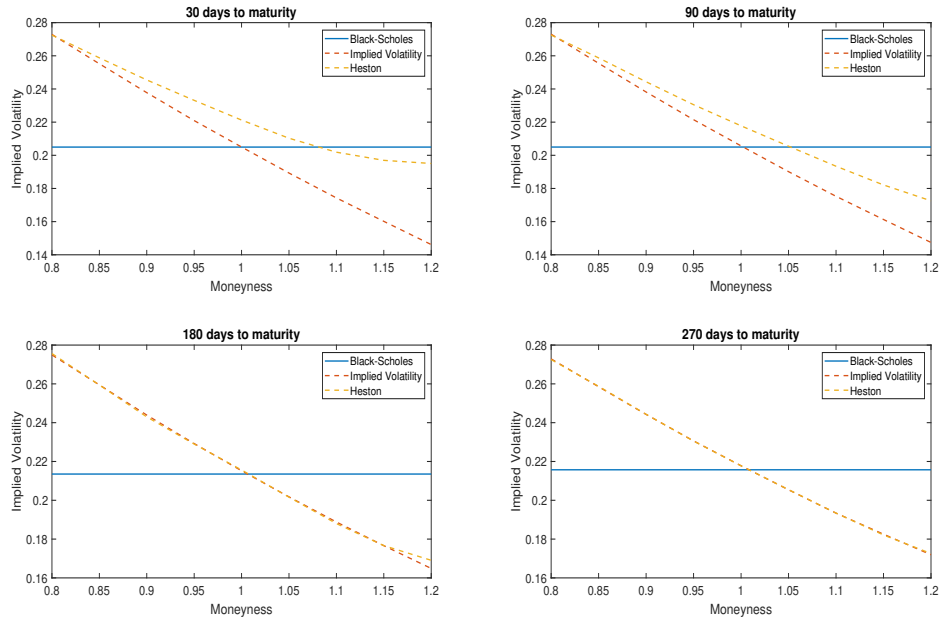
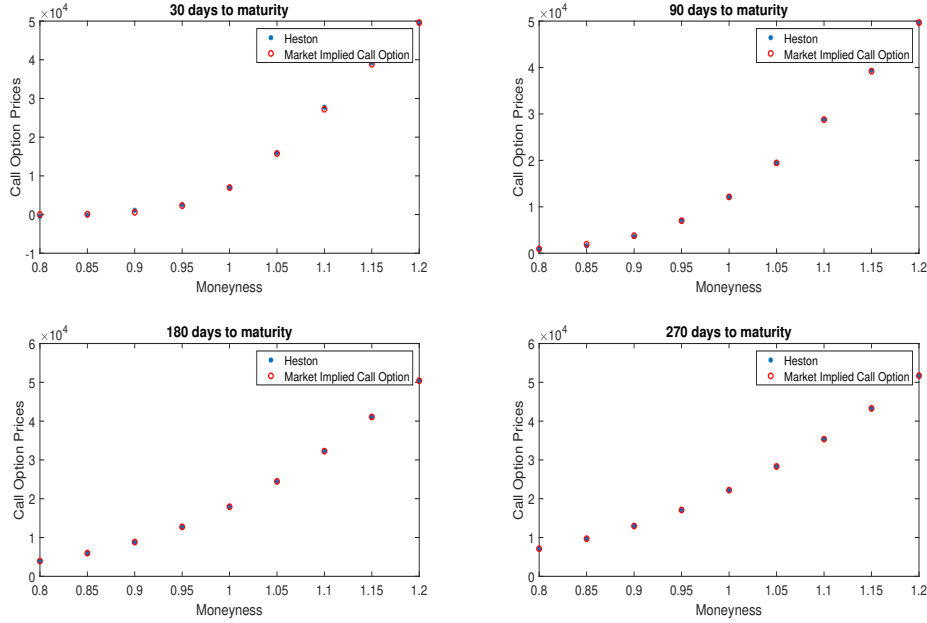


Figure 4.2: Market implied volatility smile, Heston volatility smile and BS constant volatility across various days-to-maturities.





**Figure 4.3:** Comparison of Heston and market implied call option prices across various days-to-maturities.

Recall that the Heston model is calibrated using market call option prices. The calibrated Heston call prices compared to the market call prices is shown in Figure 4.3. The corresponding Heston volatility smile is inferred from the Heston call prices. Figure 4.2 shows the Heston volatility smile compared to the market volatility smile. The deviation between the Heston volatility smile and the market volatility smile is due to the calibration on call prices.

## 4.4 Variance-Gamma Calibration

Calibration of the VG model entails determining the VG model parameters,  $\Theta_{VG} = \{\sigma_{VG}, \nu, \theta_{VG}\}$ . The VG European option price is given by,

$$\begin{aligned}
 c_t^{VG}(S_t, \tau) &= S_t P_1 - K e^{-r\tau} P_2 \\
 \text{with } P_1 &= \frac{1}{2} + \frac{1}{\pi} \sum_{n=1}^N \operatorname{Re} \left[ \frac{e^{-iu_n k} \phi_{VG}(u_n - i, \tau)}{iu_n \phi_{VG}(-i, \tau)} \right] \Delta u \\
 P_2 &= \frac{1}{2} + \frac{1}{\pi} \sum_{n=1}^N \operatorname{Re} \left[ \frac{e^{-iu_n k} \phi_{VG}(u_n, \tau)}{iu_n} \right] \Delta u,
 \end{aligned} \tag{4.3}$$

where  $\phi_{VG}(u, t)$  is given by equation (3.10),  $k = \ln(K)$ ,  $\Delta u = \frac{u_{max}}{N}$  and  $u_n = (n - \frac{1}{2})\Delta u$ . The integration limits are also truncated to the interval  $[0, u_{max}]$  with the upper integration limit  $u_{max} = 30$ , and the number of quadrature steps  $N = 100$ .

The VG calibration results are given in Table 4.3. Note that with the exception of  $\tau = 30$  days-to-maturity,  $\nu$  increases with an increase in  $\tau$ . The exception of  $\nu$  when  $\tau = 30$  days-to-maturity can be attributed to the nature of the data and ALSI market dynamics.

	Days-to-maturity			
Parameters	30	90	180	270
$\sigma_{VG}$	0.122	0.103	0.096	0.089
$\nu$	1.881	0.159	0.447	0.695
$\theta_{VG}$	0.103	0.378	0.254	0.212
RSPE	0.01	0.001	6.33e-03	4.51e-05

**Table 4.3:** VG calibrated parameters

Figure 4.4 shows the VG implied volatility smile compared to the market implied volatility smile and the Black-Scholes constant volatility. Figure 4.5 shows the VG call option prices compared to the market implied call option prices.

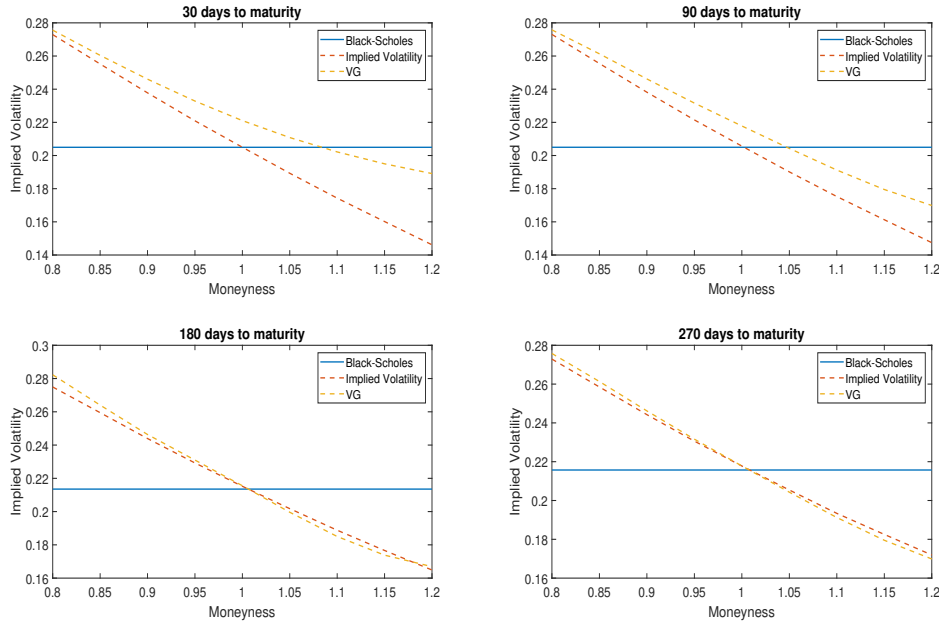


**Figure 4.4:** Market implied volatility smile, VG volatility smile and BS constant volatility across various days-to-maturities.

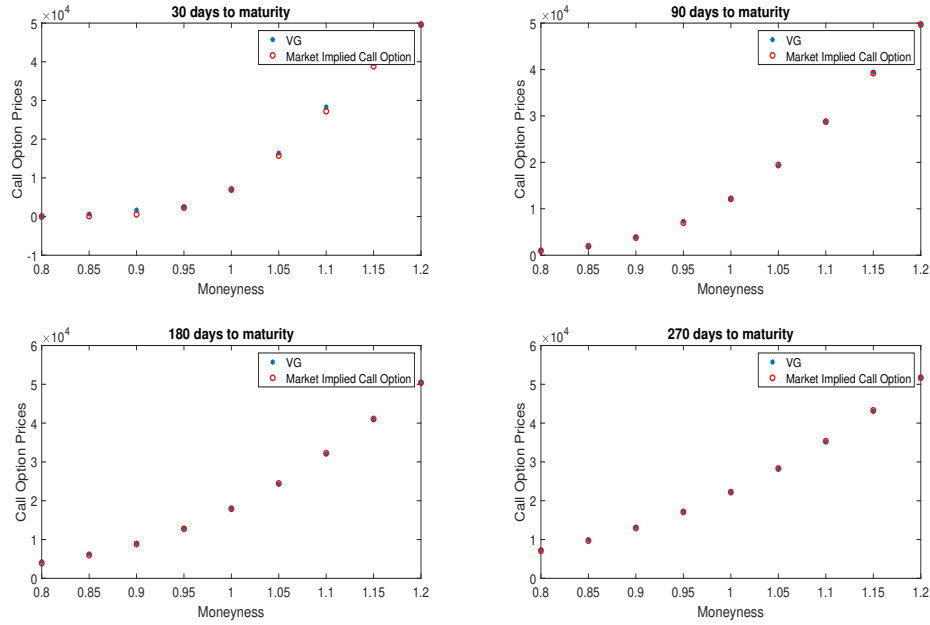


**Figure 4.5:** Comparison of VG and market implied call option prices across various days-to-maturities.

The VG model is calibrated using market call option prices. The calibrated VG call prices compared to the market call prices is shown in Figure 4.5. The corresponding Heston volatility smile is inferred from the calibration of VG prices. Figure 4.4 shows the VG volatility smile compared to the market volatility smile. The deviation between the VG volatility smile and the market volatility smile is due to the calibration on call prices.

## Chapter 5

# Static Hedging and VaR

This chapter begins with a discussion of path simulation under the real-world measure,  $\mathbb{P}$  (via a Bootstrap method) and the risk-neutral measure,  $\mathbb{Q}$ . This is followed by a discussion on static delta-hedging of European options described in Chapter 3. This is followed by a discussion of Value-at-Risk (VaR) of a portfolio under the real-world measure,  $\mathbb{P}$ , and risk-neutral measure,  $\mathbb{Q}$ . The real-world measure,  $\mathbb{P}$ , assumes the use of historical data whilst the risk-neutral measure,  $\mathbb{Q}$ , relies on risk-neutral simulation.

### 5.1 Path Simulation

The paths of the underlying are simulated via a Bootstrap method and a risk-neutral simulation. The Bootstrap method is the real-world measure,  $\mathbb{P}$ , which relies on historical data. Risk-neutral simulation is the risk-neutral measure,  $\mathbb{Q}$ , where the paths are determined in a model-dependent manner.

#### 5.1.1 Bootstrap Method

In order to simulate the sample path via bootstrap, suppose we have a historical time series of spot prices for the underlying. The daily log returns for the underlying can be obtained and denoted as  $R = [R_1, \dots, R_N]$ . That is,

$$R_i = \log \left( \frac{S_{t_i}}{S_{t_{i-1}}} \right).$$

At time  $t_0$ , we select the latest available underlying spot price as  $S_{t_0}$ . At the hedging date  $t_i \in [t_1, \dots, t_h]$  we randomly select  $R_i \in R$ . Thus,

$$S_{t_i} = S_{t_{i-1}} e^{R_i}.$$

### 5.1.2 Risk-Neutral simulation

The risk-neutral path simulation of the underlying is model dependent. In this context, the underlying follows the Black-Scholes, Heston and Variance Gamma model assumptions respectively. We begin by defining the [Milstein \(1994\)](#) approximation scheme for generating paths.

**Definition 5.1.** Milstein Approximation:

Suppose a stochastic process  $Y$  defined by,

$$dY_t = a(Y_t)dt + b(Y_t)dW_t, \quad Y_0 \text{ is a constant,}$$

where  $a, b \in C^2(\mathbb{R})$ . The [Milstein \(1994\)](#) approximation is a sequence of random variates  $\hat{Y}_0, \dots, \hat{Y}_N$  at times  $t_i$  with  $\Delta t_i = t_i - t_{i-1}$  for  $i \geq 0$  given by,

$$\hat{Y}_{t_i} = \begin{cases} Y_{t_0} & t_i = t_0, \\ \hat{Y}_{t_{i-1}} + a(\hat{Y}_{t_{i-1}})\Delta t_i + b(\hat{Y}_{t_{i-1}})\Delta W_{t_i} + \frac{1}{2}b(\hat{Y}_{t_{i-1}})\frac{db}{dx}(\hat{Y}_{t_{i-1}})((\Delta W_{t_i})^2 - \Delta t_i) & \text{otherwise,} \end{cases}$$

with  $W_t$  as the standard Brownian motion and  $\Delta W_{t_i} = W_{t_i} - W_{t_{i-1}}$ .  $\square$

Following [Glasserman \(2013\)](#), the risk-neutral sample path for the underlying under BS assumptions using Milstein approximation is given by,

$$S_{t_i} = S_{t_{i-1}} + rS_{t_{i-1}}\Delta t_i + \sigma_{BS}S_{t_{i-1}}\sqrt{\Delta t_i}Z_i + \frac{1}{2}\sigma_{BS}^2S_{t_{i-1}}(Z_i^2 - 1)\Delta t_i,$$

where  $\Delta t_i = t_i - t_{i-1}$ ,  $r$  is the risk-free rate and  $Z_i$  is a random number generated from the standard normal distribution. Similarly using the Milstein approximation, the Heston model sample path as suggested by [Rouah \(2013\)](#) and [Hirsa \(2016\)](#) is given by,

$$S_{t_i} = S_{t_{i-1}}e^{(r - \frac{1}{2}v_{t_{i-1}})\Delta t_i + \sqrt{v_{t_{i-1}}}\Delta t_i Z_{s,i}}$$

$$v_{t_i} = \max(v_{t_{i-1}} + \kappa(\theta_H - v_{t_{i-1}})\Delta t_i + \sigma_H\sqrt{v_{t_{i-1}}}\Delta t_i Z_{v,i} + \frac{1}{4}\sigma_H^2(Z_{v,i}^2 - 1)\Delta t_i, 0),$$

with  $v_0$  and  $S_0$  at hedging date  $t_0$ . The standard normal random variables  $Z_{s,i}$  and  $Z_{v,i}$  have correlation  $\rho$ .

In the case of the Variance Gamma, [Fu et al. \(2007\)](#) suggests that the sample path for an underlying is given by,

$$X_{t_i} = X_{t_{i-1}} + \theta_{VG}\Delta G_i + \sigma_{VG}\sqrt{\Delta G_i}Z_i$$

$$S_{t_i} = S_{t_{i-1}}e^{(r-\omega)\Delta t_i + X_{t_i}},$$

where  $\Delta G_i$  is a random variable generated from the Gamma distribution with shape parameter  $\frac{\Delta t_i}{\nu}$  and scale parameter  $\nu$ , whilst  $Z_i$  is a random variable generated from the standard normal distribution and  $\omega = \frac{1}{\nu} \ln(1 - \theta_{VG}\nu - 0.5\sigma_{VG}^2\nu)$ .

Figure 5.1 below shows the distributions of the underlying,  $S_{t_{10}}$ , after 10 days, assuming that one can only observe the underlying at the end of the day. The distributions of the underlying are shown for the Historical Bootstrap, BS, Heston and VG models. The distributions were fitted using MATLAB's built-in *ksdensity* function.

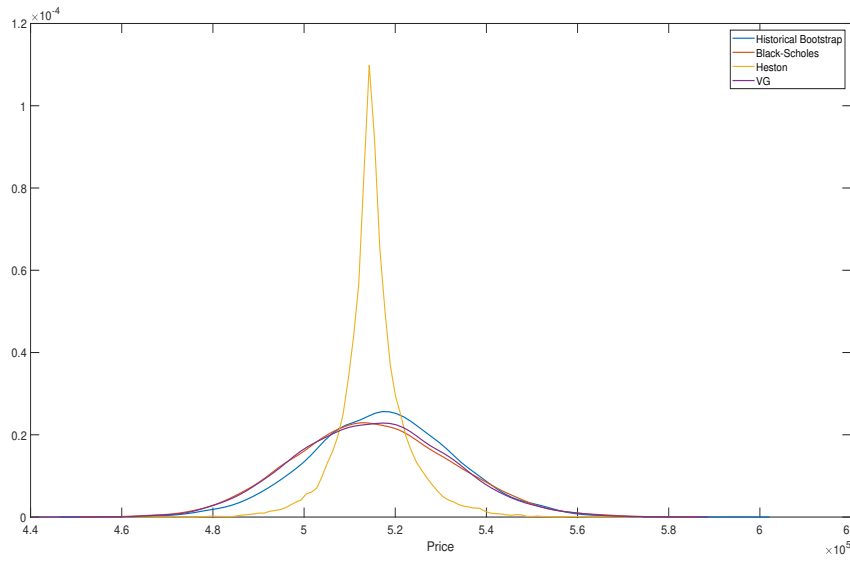


**Figure 5.1:** Distribution of  $S_{t_{10}}$  under Historical Bootstrap, Black-Scholes, Heston and Variance Gamma assumptions after 10 days.

Figure 5.1 shows that the Black-Scholes and VG underlying price distribution at time  $t_{10}$  is similar to the Historical Bootstrap distribution. The Heston distribution has a higher peak and longer tails.

## 5.2 Static Hedging

The delta of an option is regarded as the sensitivity of an option value to the change in the underlying price. The delta of a European call option, denoted  $\Delta_C$ , is defined as,

$$\Delta_C = \frac{\partial c(S_0, \tau)}{\partial S_0}. \quad (5.1)$$

Similarly the delta of a put is defined as,

$$\Delta_P = \frac{\partial p(S_0, \tau)}{\partial S_0}. \quad (5.2)$$

In the case of the Black-Scholes model, the delta of European call and put options have analytical solutions given by,

$$\Delta_C = N(d_+) \quad \text{and} \quad \Delta_P = -N(-d_+), \quad (5.3)$$

respectively where  $N(\cdot)$  is the cumulative distribution function of the standard normal distribution and  $d_+$  is given by Equation 3.3.

Similarly the delta of the Heston and VG model is found by taking the derivative of the semi-analytical formulae, given by Equations 4.2 and 4.3, with respect to  $S_0$ .

The delta of the European call and put Heston options is given by,

$$\begin{aligned} \Delta_C &= \frac{\partial c^H(S_t)}{\partial S_0} = P_1 + S_0 \frac{\partial P_1}{\partial S_0} - K e^{-r\tau} \frac{\partial P_2}{\partial S_0} \\ \Delta_P &= \frac{\partial p^H(S_t)}{\partial S_0} = S_0 \frac{\partial P_1}{\partial S_0} - (1 - P_1) - K e^{-r\tau} \frac{\partial P_2}{\partial S_0}. \end{aligned} \quad (5.4)$$

respectively where,

$$\begin{aligned} P_1 &= \frac{1}{2} + \frac{1}{\pi} \sum_{n=1}^N \operatorname{Re} \left[ \frac{e^{-iu_n \ln(K)} \phi_{Heston}(u_n - i, \tau)}{iu_n \phi_{Heston}(-i, \tau)} \right] \Delta u \\ S_0 \frac{\partial P_1}{\partial S_0} &= \frac{1}{\pi} \sum_{n=1}^N \operatorname{Re} \left[ e^{-iu_n \ln(K)} \frac{\phi_{Heston}(u_n - i, \tau)}{\phi_{Heston}(-i, \tau)} \right] \Delta u \\ \frac{\partial P_2}{\partial S_0} &= \frac{1}{\pi} \sum_{n=1}^N \operatorname{Re} \left[ \frac{e^{-iu_n \ln(K)}}{iu_n} \phi_{Heston}(u_n, \tau) \right] \Delta u. \end{aligned}$$

Similarly the delta of the European call and put options under the VG model is given by,

$$\begin{aligned} \Delta_C &= \frac{\partial c^{VG}(S_t)}{\partial S_0} = P_1 + S_0 \frac{\partial P_1}{\partial S_0} - K e^{-r\tau} \frac{\partial P_2}{\partial S_0} \\ \Delta_P &= \frac{\partial p^{VG}(S_t)}{\partial S_0} = S_0 \frac{\partial P_1}{\partial S_0} - (1 - P_1) - K e^{-r\tau} \frac{\partial P_2}{\partial S_0}. \end{aligned} \quad (5.5)$$

respectively where,

$$\begin{aligned}
P_1 &= \frac{1}{2} + \frac{1}{\pi} \sum_{n=1}^N \operatorname{Re} \left[ \frac{e^{-iu_n \ln(K)} \phi_{VG}(u_n - i, \tau)}{iu_n \phi_{VG}(-i, \tau)} \right] \Delta u \\
S_0 \frac{\partial P_1}{\partial S_0} &= \frac{1}{\pi} \sum_{n=1}^N \operatorname{Re} \left[ e^{-iu_n \ln(K)} \frac{\phi_{VG}(u_n - i, \tau)}{\phi_{VG}(-i, \tau)} \right] \Delta u \\
\frac{\partial P_2}{\partial S_0} &= \frac{1}{\pi} \sum_{n=1}^N \operatorname{Re} \left[ \frac{e^{-iu_n \ln(K)}}{iu_n} \phi_{VG}(u_n, \tau) \right] \Delta u.
\end{aligned}$$

Figure 5.2 below illustrates BS, Heston and VG delta at time  $t_0$  for the data described in Section 4.1.

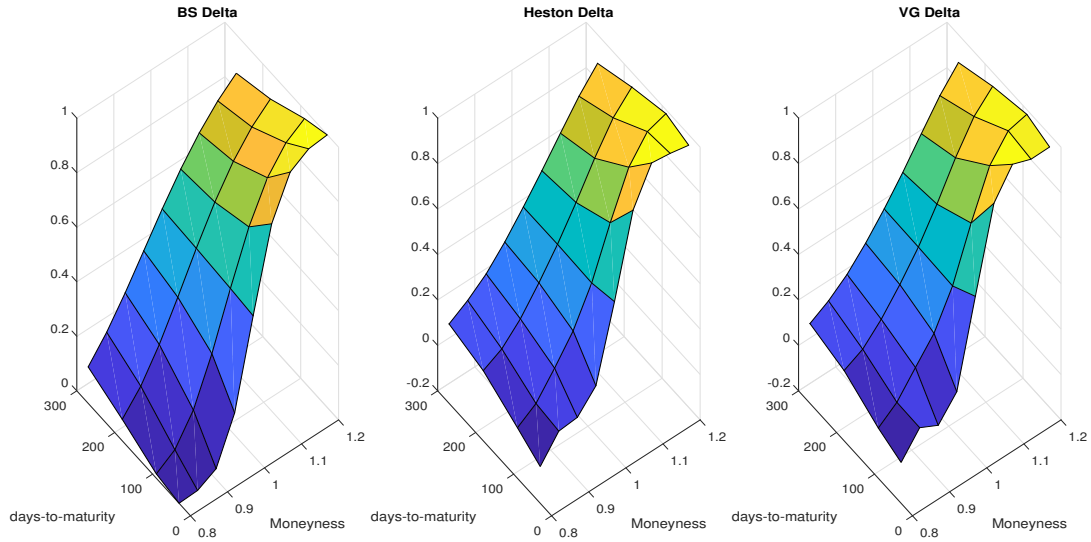


**Figure 5.2:**  $\Delta_C$  for BS, Heston and VG at time  $t_0$

The procedure for delta hedging a European call and put option is described by the following algorithm. It should be noted that this approach assumes no restrictions on the ability to long or short a financial instrument.

### Static Delta Hedging Algorithm

European call option:

1. We set up a portfolio by longing the European call option and shorting  $\Delta_C$  units of the underlying. We denote the P&L of a portfolio at time  $t$  as  $\Pi_t$  and thus, the initial residual P&L of the portfolio is given by,



$$\Pi_{t_0} = c(S_{t_0}, \tau) - \Delta_C S_{t_0}.$$

2. At time  $n$ , the Profit and Loss (P&L) is given by,

$$\Pi_{t_n} = \Pi_{t_0} e^{r\Delta t_n} + \Delta_C S_{t_n} - \Phi(S_{t_n}),$$

where  $\Phi(S_{t_n})$  denotes the value of the option at time  $t$ . That is,  $\Phi(S_T) = \max(S_T - K, 0)$  if the option is hedged until maturity.

European put option:

1. Similarly, we set up a portfolio by shorting the European put option and shorting  $\Delta_P$  units of the underlying. Therefore the initial residual P&L of the portfolio is given by,

$$\Pi_{t_0} = -|\Delta_P|S_{t_0} - p(S_{t_0}, \tau).$$

2. At time  $n$ , the P&L of the put option is given by,

$$\Pi_{t_n} = \Pi_{t_0} e^{r\Delta t_0} + |\Delta_P|S_{t_n} + \Phi(S_{t_n}).$$

It should be noted that the P&L of the European options are determined using the calibrated parameters specified in Chapter 4.

### 5.3 VaR

VaR is defined as the loss that is not expected to be exceeded with a certain significance level over a period of time. VaR was initially developed by *RiskMetrics* at JP Morgan and later became adopted by financial practitioners as a tool to measure risk (see [Guldimann et al. \(1995\)](#)).

VaR has two parameters viz.  $\alpha$ , the significance level (or the confidence level  $1 - \alpha$ ) and the risk horizon,  $h$ , which is the period of time over which VaR will be calculated. The risk horizon is the period over which one is exposed to a position. This means that the more illiquid the risk, the longer the period over which the risk should be assessed. That is, positions which cannot be closed or hedged quickly should be assessed over longer risk horizons.

Recall that the Profit and Loss (P&L) of a portfolio at time  $t_h$  is denoted by  $\Pi_{t_h}$ .  $\Pi_{t_h}$  is calculated by static hedging of European options. Let VaR be denoted as  $x_h$ . In order to estimate VaR at time  $t_h$ , we need to find the  $\alpha$ -quantile  $x_h$  such that (see [Alexander \(2009\)](#)),

$$\text{VaR}_h = -\inf\{x_h \in \mathbb{R} \mid \mathbb{P}[\Pi_{t_h} \leq x_h] \geq \alpha\}$$

We quantify the model risk inherent in the Historical VaR and Monte Carlo (MC) VaR. Historical VaR is a real-world measure,  $\mathbb{P}$  and calculated via a bootstrap method on historical data whilst MC VaR is a risk-neutral  $\mathbb{Q}$ –measure calculated by simulating the risk-neutral paths for the underlying.

## Chapter 6

# Results

Recall that this dissertation quantifies the model risk in VaR of certain portfolios by using the methodology described by [Glasserman and Xu \(2014\)](#). This methodology is used in order to compare the real-world  $\mathbb{P}$ -measure Historical VaR to the risk-neutral  $\mathbb{Q}$ -measure Monte Carlo VaR through the use of the parameter  $\delta$ . By analysing various portfolios under the change of measure, we search for  $\delta$  without solving for one. This chapter begins by analysing the Profit and Loss (P&L) distribution model risk in various portfolios based on Black-Scholes, Heston and VG models. This is followed by a discussion of the model risk in VaR under the various portfolios. The portfolios are observed over a risk horizon period of 10 days with a rate of return,  $r$ , of 7% and VaR is determined for a 95% confidence level.

The following portfolios were considered:

1. One At-The-Money (ATM) call option for each time-to-maturity.
2. Long-only portfolio with three call options with moneyness of 95%, 100% and 105% respectively.
3. Collar portfolio with a long position in an out-the-money put with a strike of 85% moneyness, short position in an out-the-money call with a strike of 115% moneyness and a long position in the ALSI future itself.

### 6.1 Profit and Loss Distributions

Recall from Chapter 2 that in order to quantify model risk, an exponential change of measure is required. The exponential change of measure is characterised by the parameter  $\delta$  and the risk measure  $V(X)$ . In our context,  $X$  refers to the P&L of the portfolio and  $V(X)$  is VaR of the portfolio.  $\mathbb{E}[m_\delta(X)V(X)]$  refers to the worst-case value of  $V(X)$  implied by the parameter  $\delta$ . In order to analyse the effect of the exponential change of measure on the MC P&L and MC VaR, various values of the parameter  $\delta$  were arbitrarily chosen. The chosen values were  $\delta = [-1.5, -0.5, 0.5, 2]$ .

Figures 6.1 - 6.3 illustrate the effect of the change of measure in order to perturb the MC P&L for the three portfolios on options with 90 days-to-maturity. The Historical and the perturbed P&L distributions for each portfolio were fitted using *MATLAB*'s built-in *ksdensity* function.

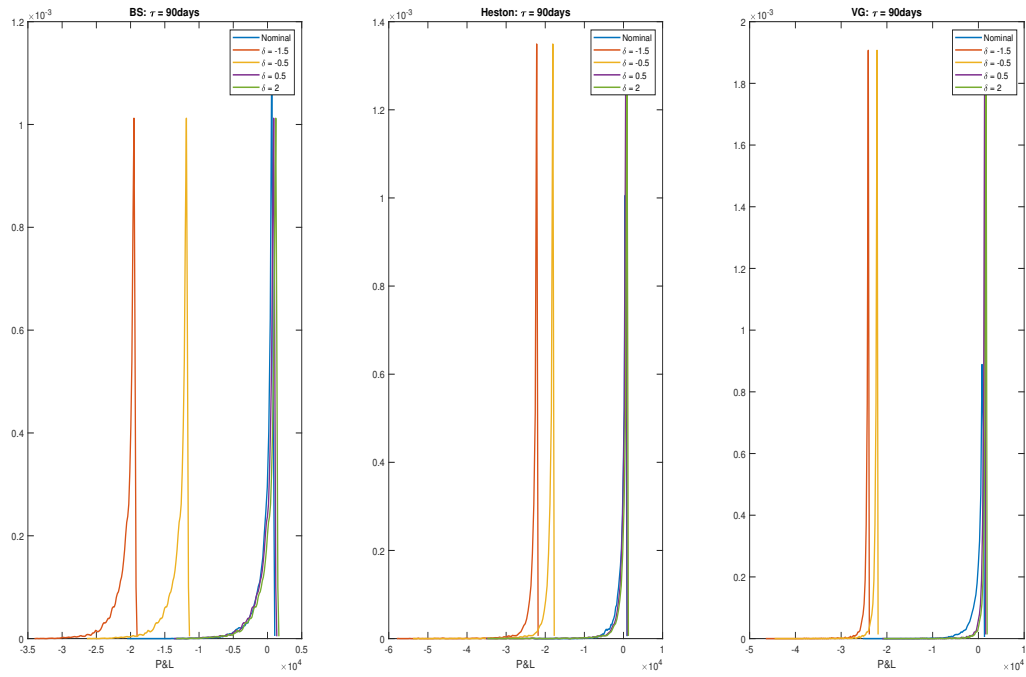


**Figure 6.1:** ATM call P&L distributions for BS, Heston and VG 90 with days-to-maturity.

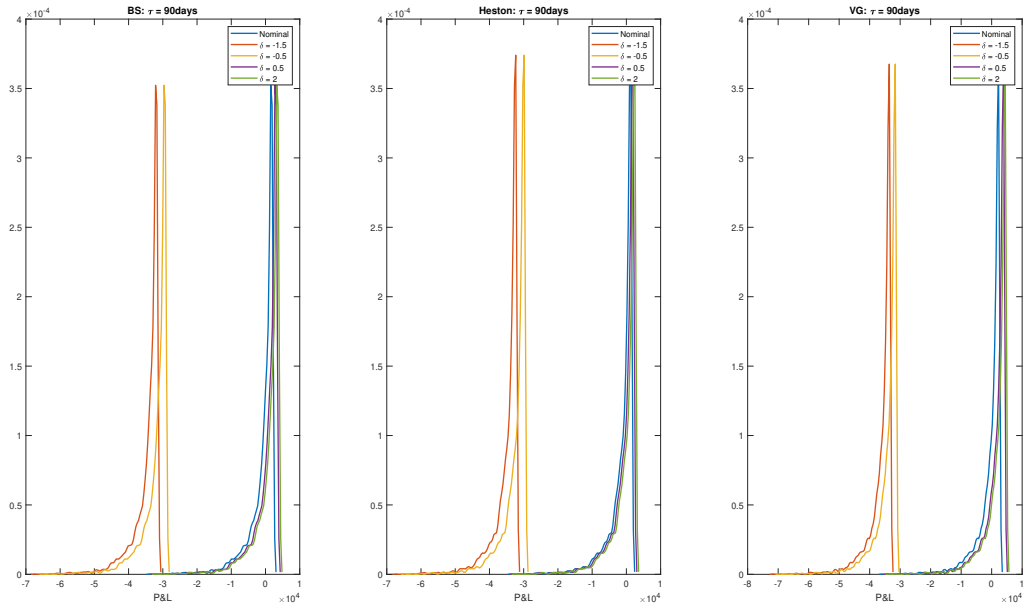


**Figure 6.2:** Long-only portfolio P&L distributions for BS, Heston and VG with 90 days-to-maturity.

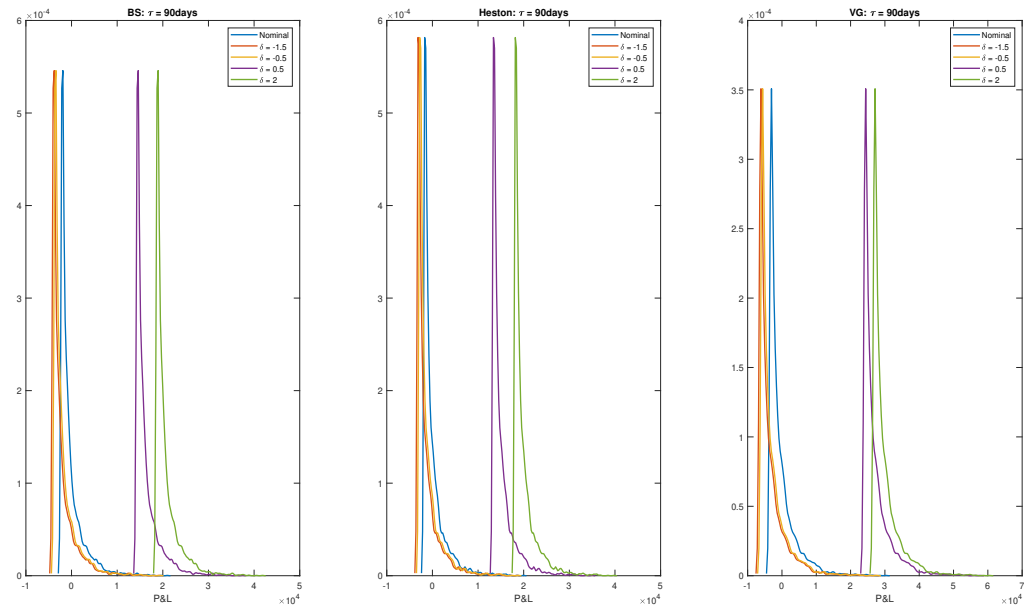


**Figure 6.3:** Collar portfolio P&L distributions for BS, Heston and VG models with 90 days-to-maturity.

Note that the parameter  $\delta$  affects some properties of the unperturbed MC P&L distribution. The  $\delta$  shifts the distributions for each portfolios. The change of measure on the respective P&L distributions changes the moments of the distributions. If  $\delta$  can be interpreted as a pseudo-risk aversion measure, then  $\delta < 0$  can be interpreted as some level of risk aversion and the worst-case shifts the profitability towards a loss. On the other hand,  $\delta > 0$  can be interpreted as a level of risk-taking and shifts the P&L in the opposite direction.

It should be noted that  $\delta < 0$  does not have a symmetric effect on the P&L distribution as  $\delta > 0$ . Similarly, the effect of  $\delta$  varies with each portfolio.

The effect of the exponential change of measure for portfolios on options with 30, 180 and 270 days-to-maturity is presented in Figures B.1 - B.3, B.4-B.6 and B.7-B.9 respectively.

## 6.2 VaR model risk

Recall from Section 5.3 that Historical and Monte Carlo VaR was obtained by bootstrapping and simulating the risk-neutral sample paths respectively. Table 6.1 presents the 95% VaR over a 10 day period, for the various portfolios consisting of options with 90 days-to-maturity for Black-Scholes, Heston and VG, respectively.

	$\tau = 90$	BS	Heston	VG
ATM	Historical	3 429.00	3 432.41	3 316.15
	Monte Carlo	3 712.18	3 130.73	593.97
Long Only	Historical	9 530.04	9 492.48	8 963.50
	Monte Carlo	10 428.54	8 612.07	2 007.54
Collar	Historical	2 171.70	1 737.83	3 339.13
	Monte Carlo	2 171.50	1 739.41	3 344.06

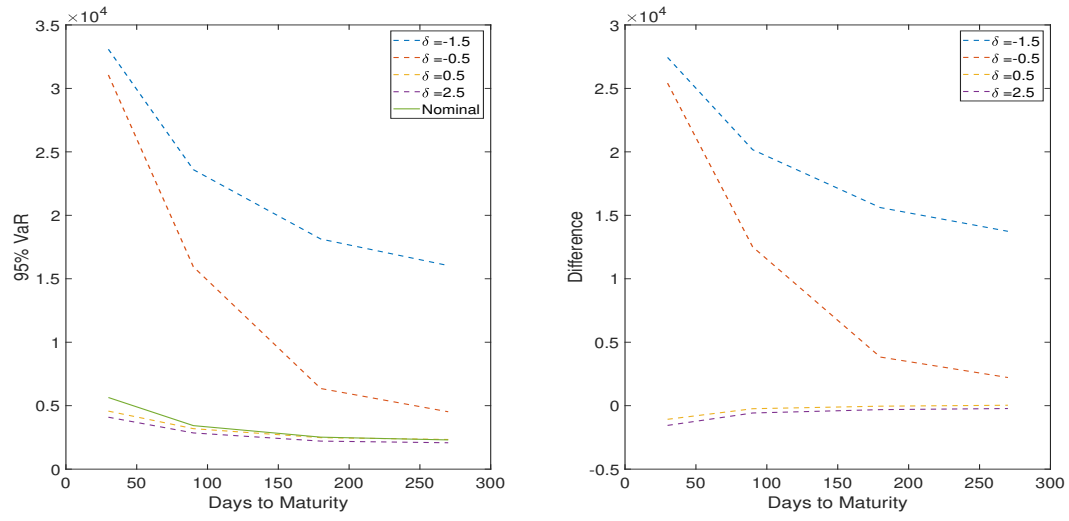
**Table 6.1:** 10-day VaR of portfolios with  $\tau = 90$  days-to-maturity

From Table 6.1 above, Black-Scholes and Heston Monte Carlo VaR is commensurate with its Historical VaR. With the exception of the collar portfolio, there is a disparity between the VG Monte Carlo VaR and the Historical VaR. VaR of portfolios with 30, 180, 270 days-to-maturity exhibit similar results and are given in Tables B.1 - B.3.

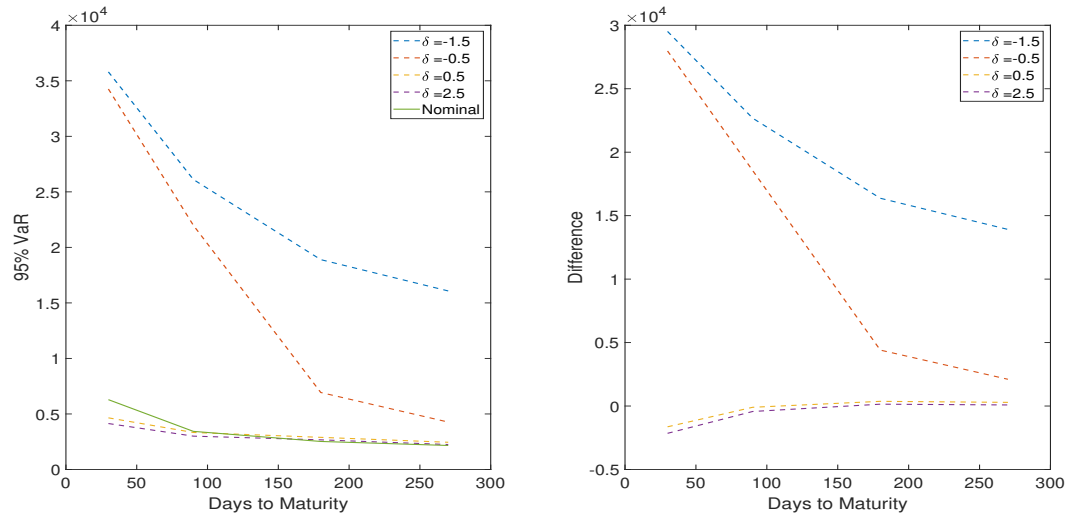
Figure 6.4 illustrates the effect on VaR on an ATM portfolio under the change of measure and the difference between the nominal distribution and the perturbed VaR. The effect of the exponential change of measure can be seen in the values of

the difference at each day-to-maturity. The greatest difference across the stochastic models occurs for options with 30 days-to-maturity, for each  $\delta$ . Under each stochastic model and for each day-to-maturity,  $\delta = 0.5$  gives the least difference.

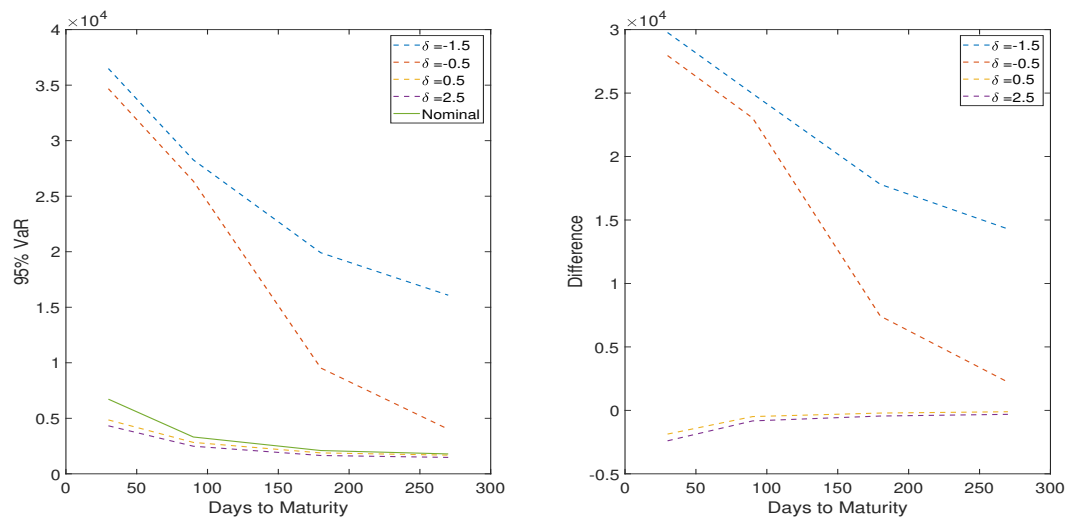
Similarly, Figures 6.5 and 6.6 illustrate the effect of the parameter  $\delta$  on VaR, based on a long-only and collar portfolio respectively, including the differences between the nominal VaR and perturbed VaR. For a long position in an ATM call and the long-only portfolio,  $\delta = 0.5$  provides a commensurate perturbed MC VaR whilst  $\delta = -0.5$  provides a commensurate perturbed collar MC VaR.



(a) BS: 95% VaR



(b) Heston 95% VaR



(c) VG: 95% VaR

Figure 6.4: ATM Nominal and Perturbed MC 95% VaR



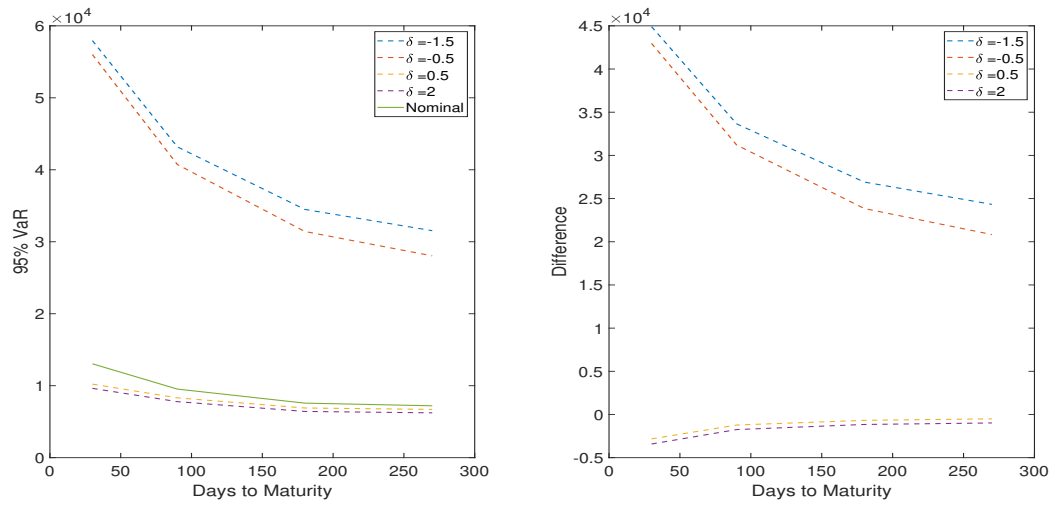
It is worth noting that the change of measure has an effect on VaR dependent on the portfolio, time-to-maturity and parameter  $\delta$ .

Recall from Section 2.1 the model risk classification which provides a framework in which model risk in the various portfolios can be attributed to a variety of factors. These are:

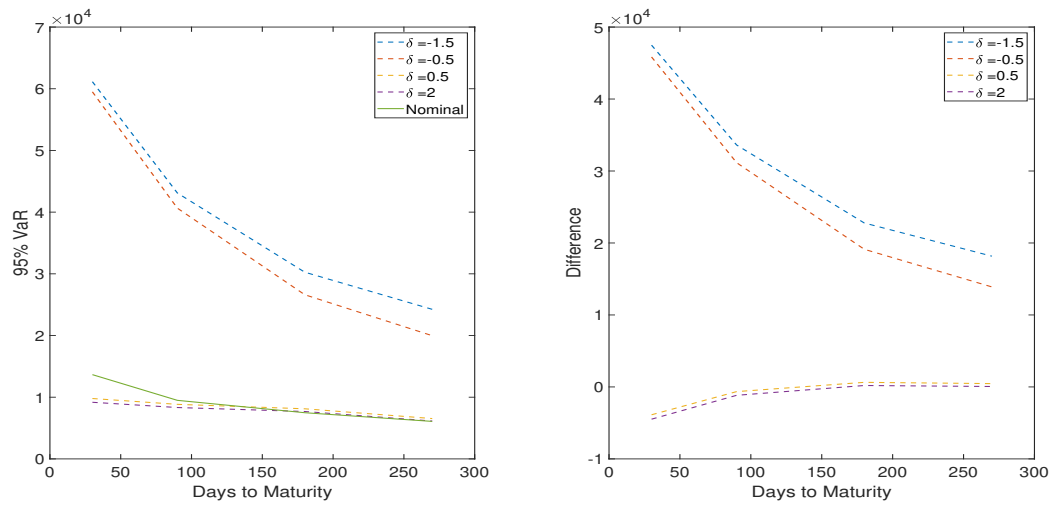
- the sparse available data. That is, the ALSI options data obtained only consists of [30, 90, 180, 270] days-to-maturity
- the initial assumptions regarding the assumptions about the underlying's stochastic behaviour
- truncating the integration limits during valuation and calibration of the Heston and VG models
- using the initial calibration parameters throughout the risk horizon period. That is, not recalibrating the parameters and thus assuming the calibrated parameters give an ideal representation of the dynamics throughout the risk horizon period.

The first factor, which is termed calibration error, can be seen in Figures 4.2 and 4.4. The calibrated parameters for 30 and 90 days-to-maturity does not seem to retrieve the market implied volatility smile for the Heston and VG models. The model risk regarding the use of semi-analytical formulae of the delta is implied in Figure 5.2.

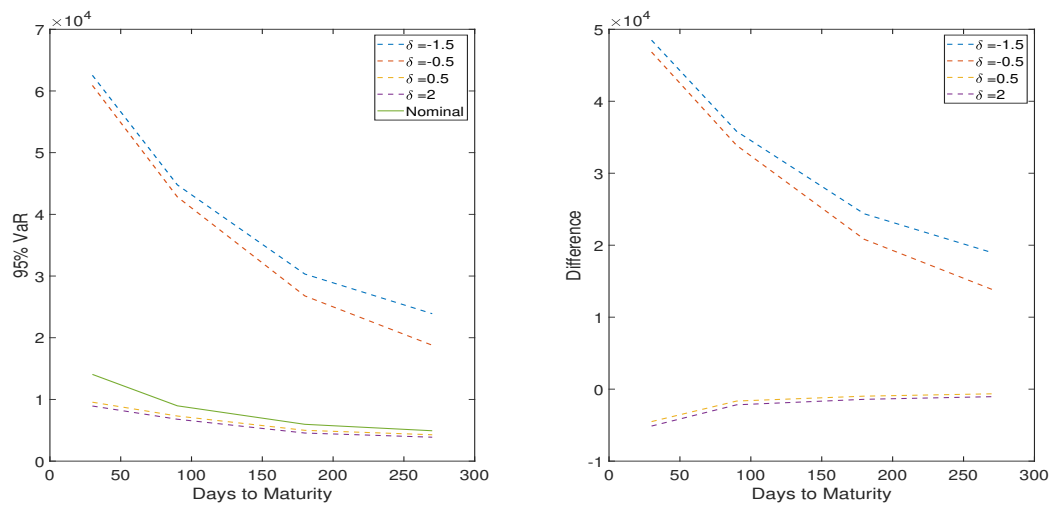
Recall that the aim of the dissertation is to quantify the effect of the exponential measure on VaR of the various portfolios and not to quantify the model risk pertaining to each risk factor. Figures 6.4 - 6.6 implicitly shows the effect of the exponential change of measure. By analysing the difference between the nominal and the perturbed MC VaR for BS, Heston and VG, the biggest difference is found at 30 days-to-maturity. This could be due to the above-mentioned calibration error or the compounded effect from a combination of various risk factors.



(a) BS: 95% VaR

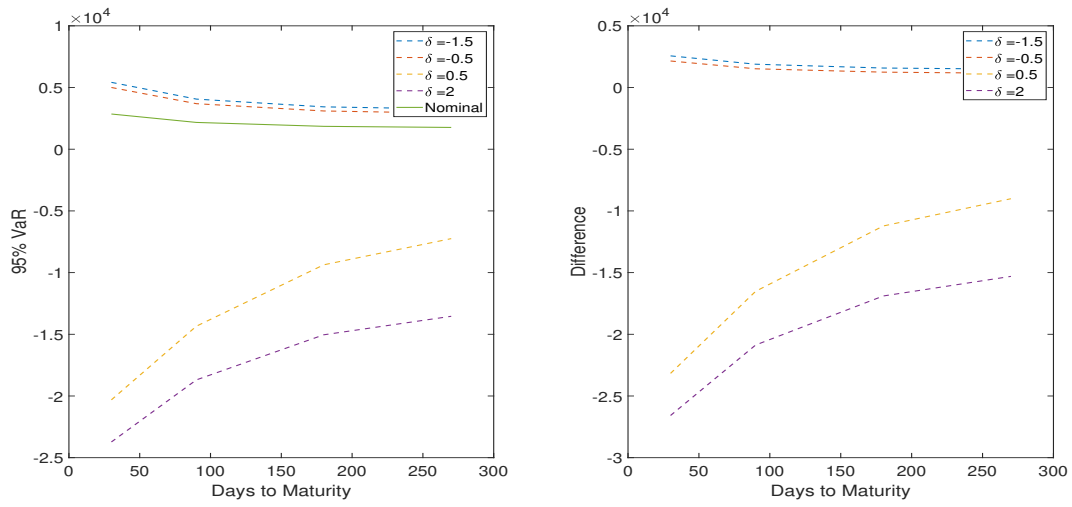


(b) Heston 95% VaR

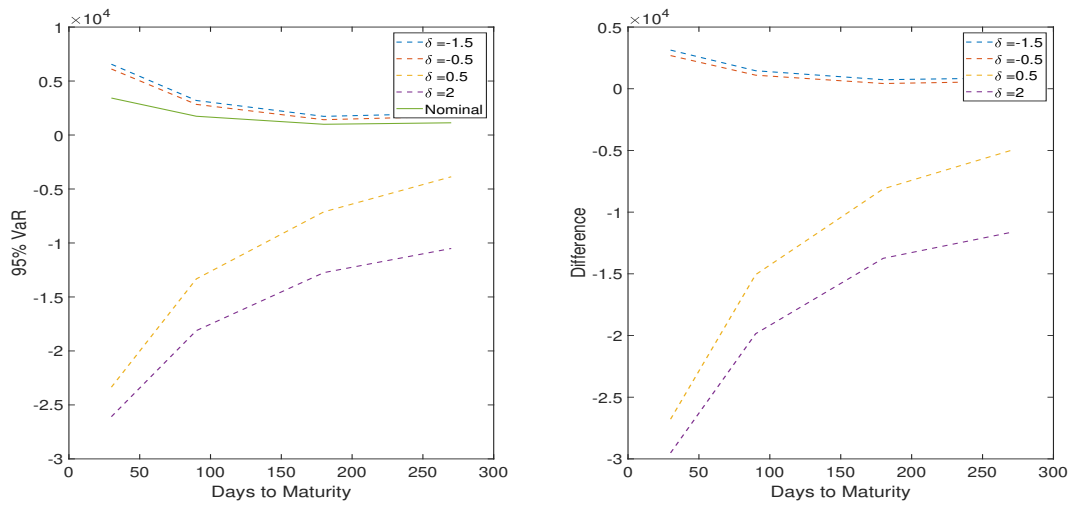


(c) VG: 95% VaR

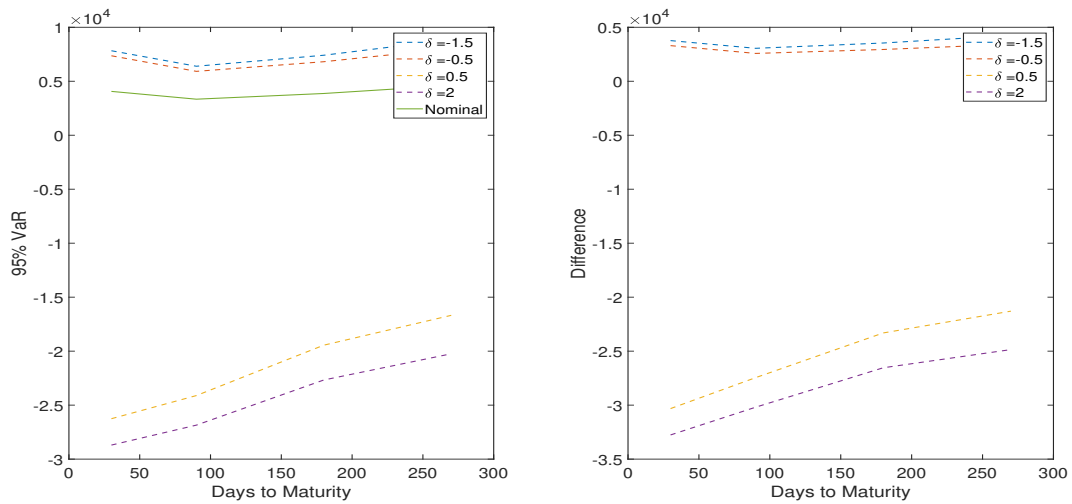
Figure 6.5: Long-only Nominal and Perturbed MC 95% VaR



(a) BS: 95% VaR



(b) Heston 95% VaR



(c) VG: 95% VaR

Figure 6.6: Collar Nominal and Perturbed MC 95% VaR

## Chapter 7

# Discussion and Conclusion

In this section, the results throughout the dissertation are discussed and concluding remarks are presented.

The calibration results of the Black-Scholes, Heston and Variance-Gamma models were presented in Chapter 4. Calibration of Black-Scholes, Heston and VG reflected European option prices similar to the market implied prices for options with times-to-maturity of [30, 90, 180, 270] days.

We implemented static delta hedging in order to obtain the model-dependent P&L distributions. The delta of the Heston and VG models was obtained from the semi-analytical formulae, whilst the closed-form analytical formula of the delta was used for the BS model. The resultant P&L distributions were presented in Section 6.1 for each portfolio on BS, Heston and VG European options using four arbitrary values of  $\delta$  in order to analyse the effect of the exponential change of measure on the P&L distributions. The results suggest that  $\delta$  can be interpreted as a pseudo risk-aversion measure. The effect of  $\delta$  was shifting the P&L distributions, in particular  $\delta < 0$  shifted the distribution to the left and  $\delta > 0$  had the opposite effect. This was seen across the various portfolios and days-to-maturity.

The effect of the exponential change of measure was observed on VaR of the various portfolios and the results were presented in Section 6.2. The exponential change of measure had various effects on the worst-case VaR for each  $\delta$ . The pseudo risk-aversion measure of  $\delta = [0.5, 2]$  for ATM and long-only option portfolios across the BS, Heston and VG models illustrated the least deviation from the nominal model. In contrast, a pseudo risk-aversion measure of  $\delta = [-0.5, -1.5]$  for the collar portfolio across the BS, Heston and VG models had the least deviation from the nominal model. This suggests that for regular option portfolios, one is afforded the flexibility of being less risk-averse without added financial implications.

Some risk factors contributing to the model error were identified using the model risk classification framework (see Schlögl (2016)). These include the use of sparse data during calibration and using the calibrated parameters to simulate the

sample paths without recalibrating to find the parameters describing each day. Recall that model risk provides a framework that enables one to compare models and inherent risk. However the aim of this dissertation was not to quantify the model risk attributed to each risk factor. That is, the idiosyncratic effect for each type of model risk described by the model risk framework was not quantified.

In conclusion, quantification of the worst-case model error presents an alternative method to model risk. This is evident in the results of VaR on the various portfolios. The use of  $\delta$  allows one to quantify the pseudo risk-aversion measure and the precise value of the pseudo risk-aversion measure  $\delta$  should be at the discretion of the practitioner. Model risk quantification and the model risk framework are recommended as they illustrate the risks implicitly inherent in a model in comparison to another model and presents a framework which classifies various risks.

The model risk framework presents an opportunity for further investigation on alternative risk metrics such as Expected Shortfall or VaR on complex financial products, such as basket options. Complex option portfolios might be of regulatory interest as market data for these are not readily available. Regulatory bodies might be concerned with various internal models used to calculate historical VaR. These internal models might be subject to model error and quantifying the worst-case model error might be beneficial in developing a robust regulatory framework.

# Bibliography

- Albrecher, H., Mayer, P., Schoutens, W. and Tistaert, J. (2007). The Little Heston Trap, *Wilmott Magazine* (1): 83–92.
- Alexander, C. (2009). *Market Risk Analysis, Value at Risk Models*, Vol. 4, John Wiley & Sons.
- Black, F. and Scholes, M. (1973). The Pricing of Options and Corporate Liabilities, *Journal of political economy* **81**(3): 637–654.
- Carr, P. and Madan, D. (1999). Option Valuation Using the Fast Fourier Transform, *Journal of computational finance* **2**(4): 61–73.
- Cox, J., Ingersoll Jr, J. and Ross, S. (1985). A theory of the term structure of interest rates, *Econometrica* **53**(2): 395–408.
- Cui, Y., del Baño. Rollin, S. and Germano, G. (2017). Full and Fast Calibration of the Heston Stochastic Volatility Model, *European Journal of Operational Research* **263**(2): 625–638.
- Derman, E. (1996). Model Risk: What Are the Assumptions Made in Using Models to Value Securities and What Are the Consequent Risks, *London: Risk Magazine* **9**: 34–38.
- Detering, N. and Packham, N. (2016). Model Risk of Contingent Claims, *Quantitative Finance* **16**(9): 1357–1374.
- Escobar, M. and Gschnaidtner, C. (2016). Parameters Recovery Via Calibration in the Heston Model: A Comprehensive Review, *Wilmott* **2016**(86): 60–81.
- Fu, M., Jarrow, R., Yen, J.-Y. and Elliott, R. (2007). *Advances in Mathematical Finance*, Springer Science & Business Media.
- Gil-Pelaez, J. (1951). Note on the Inversion Theorem, *Biometrika* **38**(3-4): 481–482.
- Glasserman, P. (2013). *Monte Carlo Methods in Financial Engineering*, Springer Science & Business Media.
- Glasserman, P. and Xu, X. (2014). Robust Risk Measurement and Model Risk, *Quantitative Finance* **14**(1): 29–58.
- Guldimann, T., Zangari, P., Longerstaey, J., Matero, J. and Howard, S. (1995). Risk-metrics Technical Document, *Morgan Guaranty Trust Company*.

- Hansen, L. and Sargent, T. (2008). *Robustness*, Princeton university press.
- Heston, S. L. (1993). A Closed-form Solution for Options With Stochastic Volatility With Applications to Bond and Currency Options, *The review of financial studies* 6(2): 327–343.
- Hirsa, A. (2016). *Computational Methods in Finance*, 1 edn, CRC Press.
- Kerkhof, J., Melenberg, B. and Schumacher, H. (2010). Model Risk and Capital Reserves, *Journal of Banking & Finance* 34(1): 267–279.
- Kullback, S. and Leibler, R. (1951). On Information and Sufficiency, *The Annals of mathematical statistics* 22(1): 79–86.
- Madan, D., Carr, P. and Chang, E. (1998). The Variance Gamma Process and Option Pricing, 2(1): 79–105.
- Milstein, G. (1994). *Numerical Integration of Stochastic Differential Equations*, Springer Science & Business Media.
- Rouah, F. (2013). *The Heston Model and Its Extensions in Matlab and C*, John Wiley & Sons.
- Schlögl, E. (2016). Toward Quantifying Model Risk.

## Appendix A

# Preliminaries

### A.1 Definitions

**Definition A.1.** A metric,  $d(\cdot, \cdot) : \mathbb{R}^n \times \mathbb{R}^n \rightarrow \mathbb{R}^+$  is defined as

$$d(x, y) = \|x - y\|_2 = \sqrt{(x_1 - y_1)^2 + \cdots + (x_n - y_n)^2},$$

which satisfies the following conditions:

- i  $d(x, y) \geq 0$ , for all  $x, y \in \mathbb{R}^n$ ,
- ii  $d(x, y) = 0$ , if and only if  $x = y$ ,
- iii  $d(x, y) = d(y, x)$ , for all  $x, y \in \mathbb{R}^n$ ,
- iv  $d(x, z) \leq d(x, y) + d(y, z)$  for all  $x, y, z \in \mathbb{R}^n$ .

### A.2 Lagrangian Duality

Consider the primal problem,

$$p_0 = \inf_m f(m) \quad \text{subject to} \quad g(m) \leq 0. \quad (\text{A.1})$$

Define

$$J(m) = \begin{cases} f(m), & \text{if } g(m) \leq 0 \\ \infty, & \text{else.} \end{cases}$$

Then equation A.1 is equivalent to  $p_0 = \inf_m J(m)$ . Define the Lagrangian,

$$L(m, \lambda) := f(m) + \lambda g(m).$$

Then,

$$\sup_{\lambda \geq 0} L(m, \lambda) = \begin{cases} f(m), & \text{if } g(m) \leq 0 \\ \infty, & \text{else.} \end{cases} = J(m),$$

and hence A.1 is equivalent to  $p_0 = \inf_m \sup_{\lambda \geq 0} L(m, \lambda)$ . The dual problem is then defined as  $d_0 = \sup_{\lambda \geq 0} \inf_m L(m, \lambda)$ . It can easily be seen that  $d_0 \leq p_0$ : We



have  $L(m, \lambda) \leq J(m)$  for all  $\lambda$ , so that  $\inf_m L(m, \lambda) \leq J(m) = p_0$  and hence  $d_0 \leq p_0$ . If the optimisation problem is convex, then  $d_0 = p_0$ .

Following similar reasoning as above, the primal problem is redefined as

$$p_0 = \inf_m f(m) \quad \text{subject to} \quad g(m), \quad (\text{A.2})$$

with the dual problem,

$$d_0 = \sup_{\lambda \in \mathbb{R}} \inf_m L(m, \lambda).$$

Similarly, a mixture primal of the form,

$$p_0 = \inf_m f(m) \quad \text{subject to} \quad g(m) \leq 0 \quad \text{and} \quad h(m) = 0,$$

has the dual problem,

$$d_0 = \sup_{\lambda \geq 0, \mu \in \mathbb{R}} \inf_m L(m, \lambda, \mu),$$

where  $L(m, \lambda, \mu) := f(m) + \lambda g(m) + \mu h(m)$ . Maximisation problems  $\max_m f(m)$  can be solved by minimising  $-f(m)$ .

## Appendix B

# Appendix B

### B.1 Profit and Loss Distributions

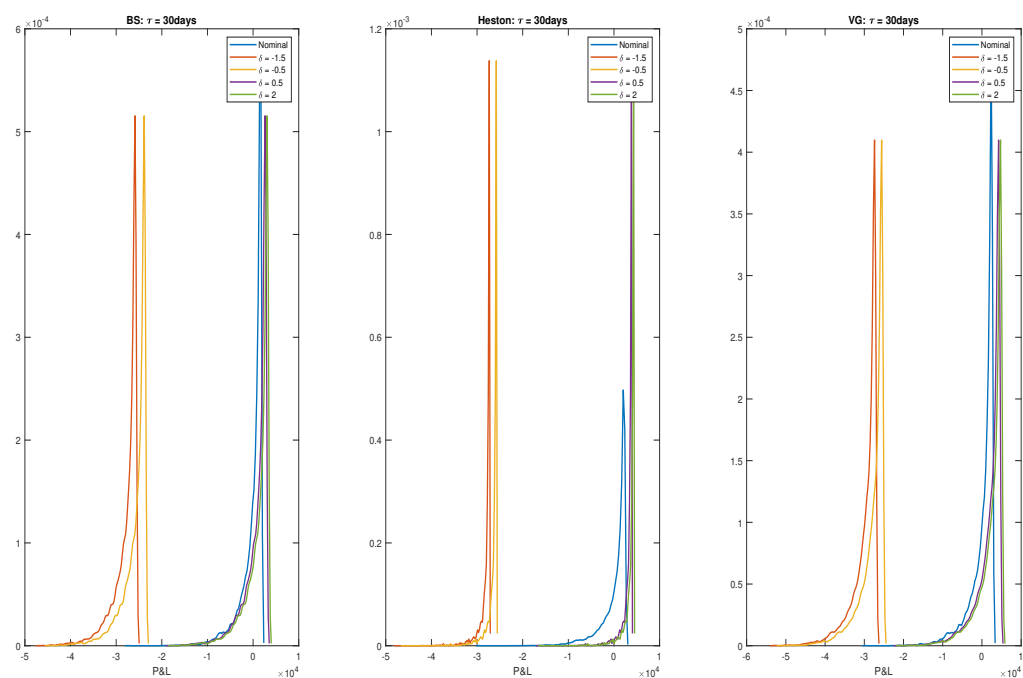


**Figure B.1:** ATM portfolio nominal and perturbed P&L Distributions for the BS, Heston and VG models 30 days-to-maturity options.

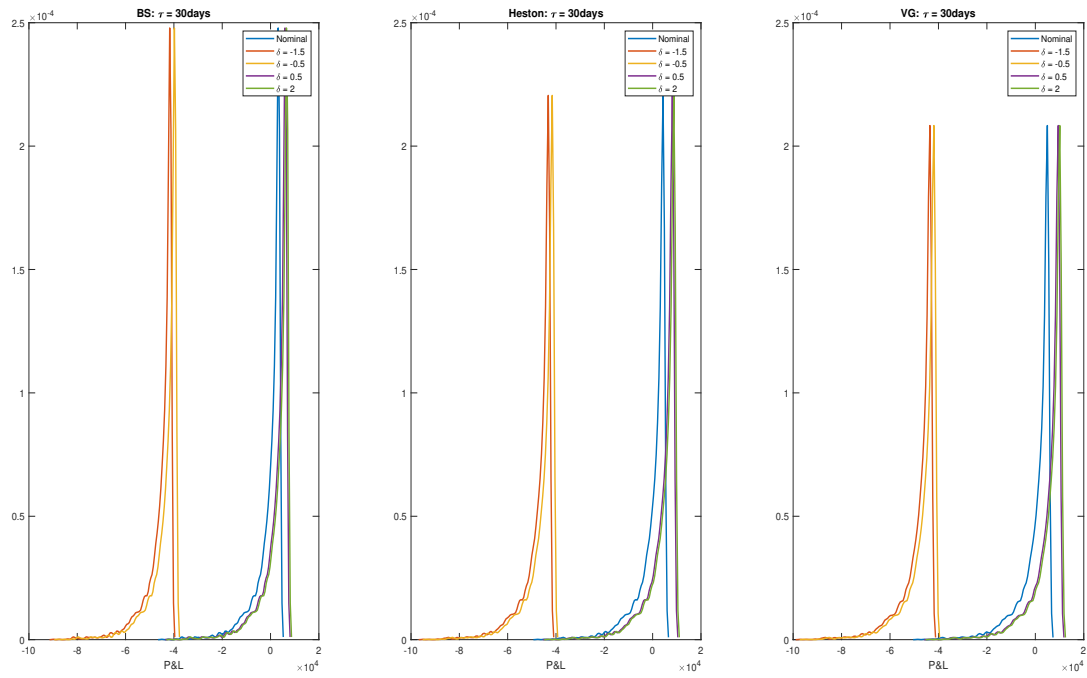


**Figure B.2:** Long-only portfolio nominal and perturbed P&L Distributions for the BS, Heston and VG models 30 days-to-maturity options.

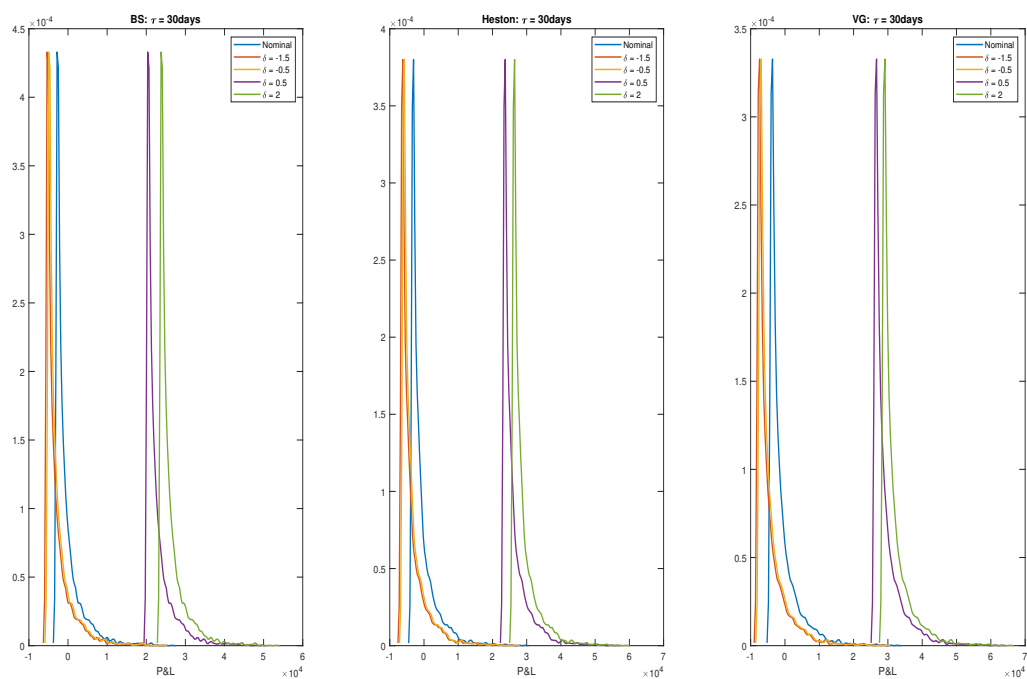


**Figure B.3:** Collar portfolio nominal and perturbed P&L Distributions for the BS, Heston and VG models 30 days-to-maturity options.

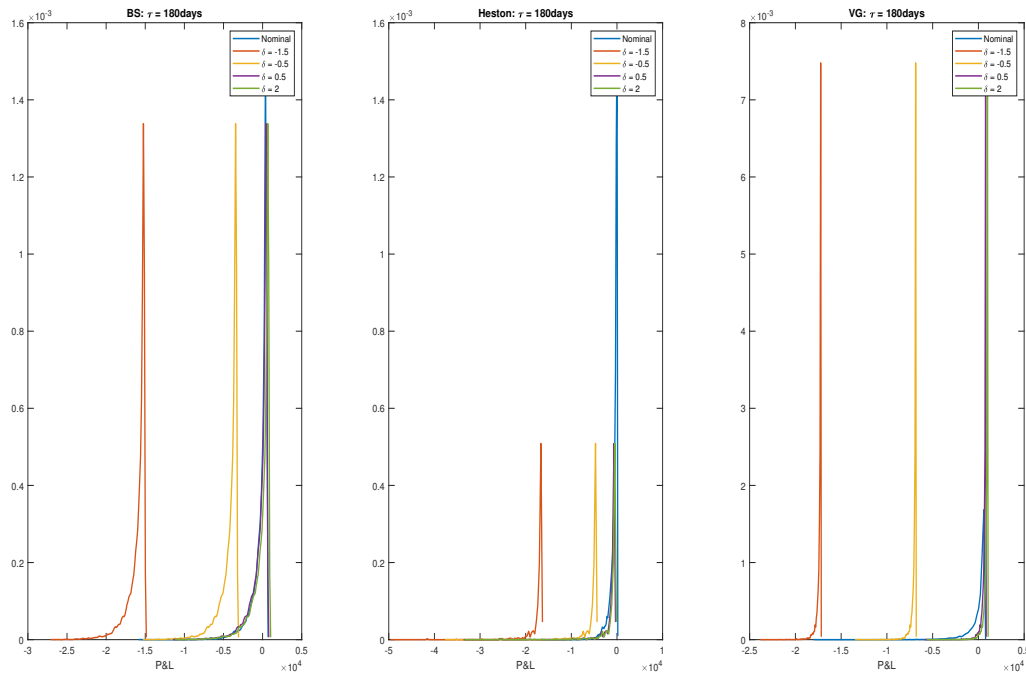


**Figure B.4:** ATM portfolio perturbed P&L Distributions for the Black-Scholes (BS), Heston and VG models 180 days-to-maturity options.

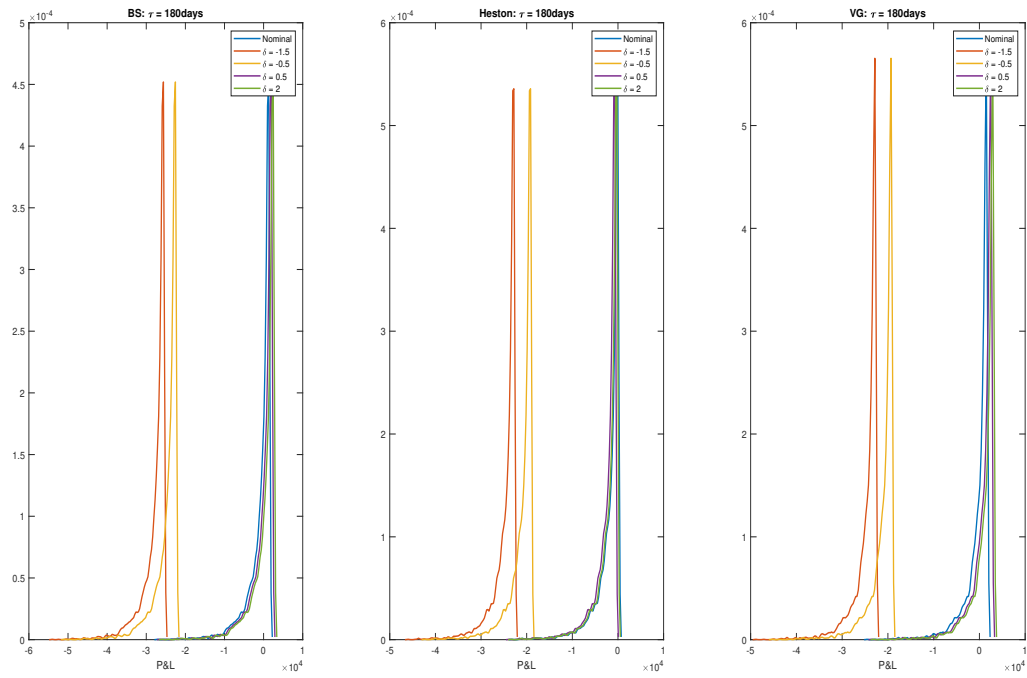


**Figure B.5:** Long-only portfolio perturbed P&L Distributions for the Black-Scholes (BS), Heston and VG models 180 days-to-maturity options.

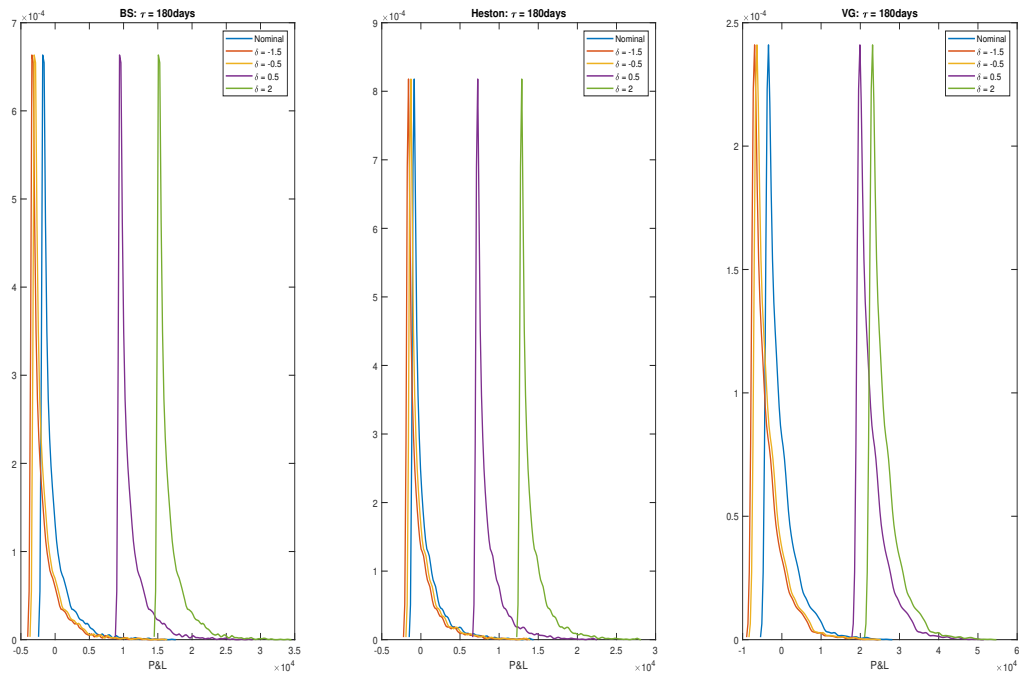


**Figure B.6:** Collar portfolio perturbed P&L Distributions for the Black-Scholes (BS), Heston and VG models 180 days-to-maturity options.

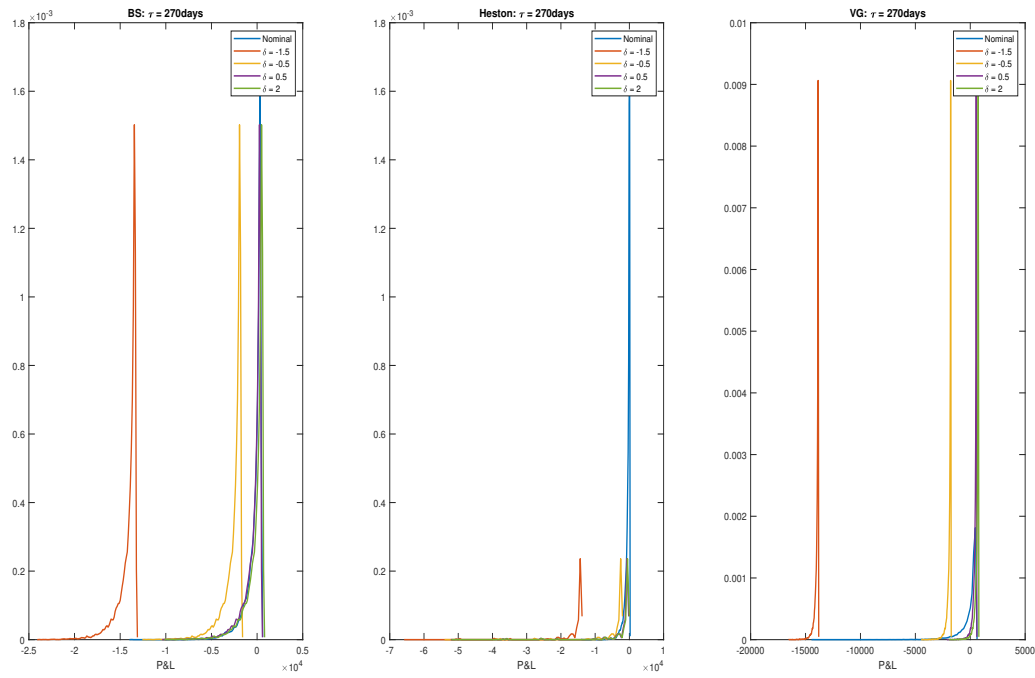


**Figure B.7:** ATM portfolio perturbed P&L Distributions for the Black-Scholes (BS), Heston and VG models 270 days-to-maturity options.



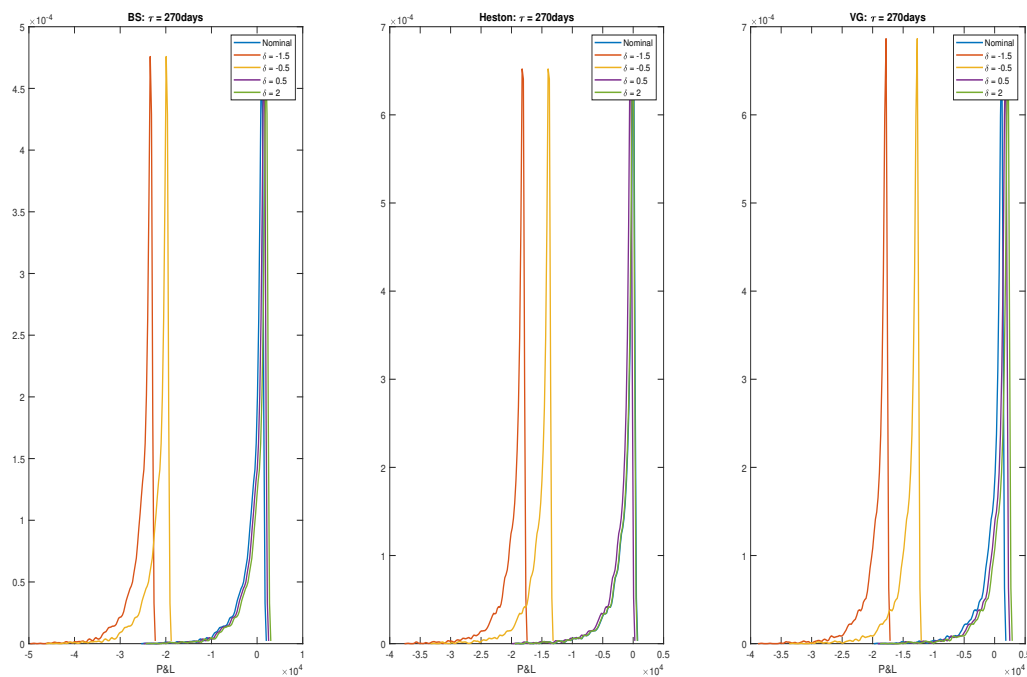


**Figure B.8:** Long-only portfolio perturbed P&L Distributions for the Black-Scholes (BS), Heston and VG models 270 days-to-maturity options.

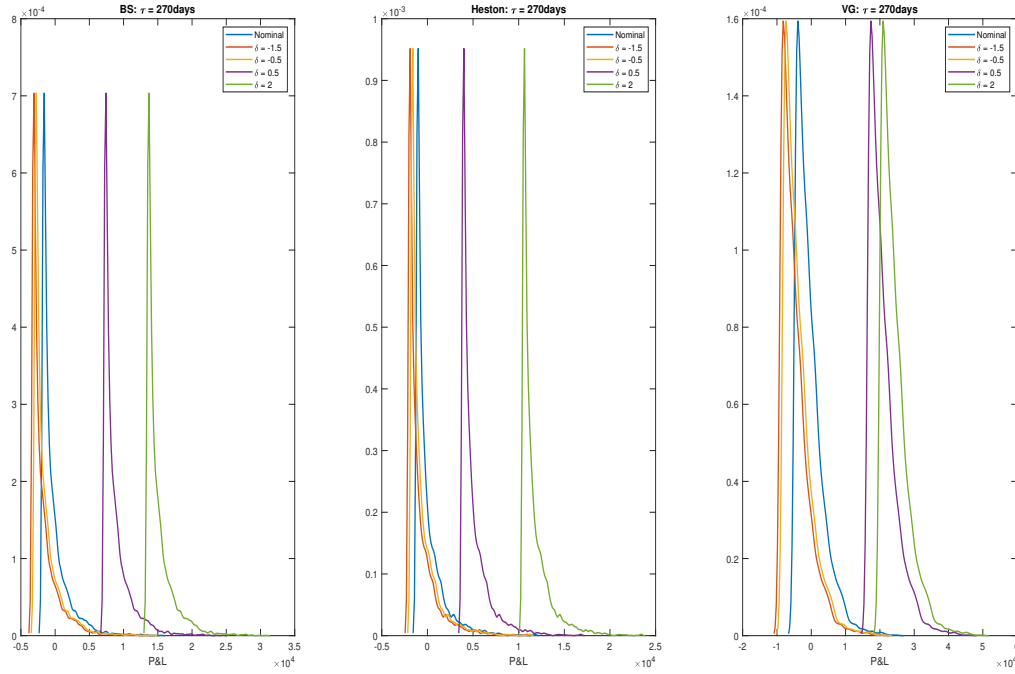


**Figure B.9:** Collar portfolio perturbed P&L Distributions for the Black-Scholes (BS), Heston and VG models 270 days-to-maturity options.

## B.2 VaR Results

	$\tau = 300$	BS	Heston	VG
ATM	Historical	5644.24	6287.62	6723.06
	Monte Carlo	6157.33	189.17	7175.31
Long Only	Historical	13045.07	13657.44	14058.28
	Monte Carlo	14697.12	266.33	15764.18
Collar	Historical	2853.12	3425.23	4061.27
	Monte Carlo	2854.37	3435.95	4060.94

**Table B.1:** 10-day VaR of portfolios with  $\tau = 30$  days-to-maturity

	$\tau = 270$	BS	Heston	VG
ATM	Historical	2302.03	2162.04	1791.75
	Monte Carlo	2702.26	2183.09	49.25
Long Only	Historical	7208.47	6079.4	4922.17
	Monte Carlo	8206.81	6237.31	274.63
Collar	Historical	1765.37	1132.05	4611.95
	Monte Carlo	1765.42	1122.75	3913.78

**Table B.3:** 10-day VaR of portfolios with  $\tau = 270$  days-to-maturity

	$\tau = 180$	BS	Heston	VG
ATM	Historical	2520.12	2523.94	2097.28
	Monte Carlo	2943.49	1799.37	119.98
Long Only	Historical	7580.47	7485.51	5966.66
	Monte Carlo	8781.13	5402.23	600.51
Collar	Historical	1853.99	994.37	3866.77
	Monte Carlo	1852.88	991.66	3751.11

**Table B.2:** 10-day VaR of portfolios with  $\tau = 180$  days-to-maturity